



January 2013

Preparation And Characterization Of Meridionally Trischelated Rhenium(i) Terpyridine Dicarbonyl Complexes

Daniel Black

Follow this and additional works at: <https://commons.und.edu/theses>

Recommended Citation

Black, Daniel, "Preparation And Characterization Of Meridionally Trischelated Rhenium(i) Terpyridine Dicarbonyl Complexes" (2013). *Theses and Dissertations*. 1401.
<https://commons.und.edu/theses/1401>

This Thesis is brought to you for free and open access by the Theses, Dissertations, and Senior Projects at UND Scholarly Commons. It has been accepted for inclusion in Theses and Dissertations by an authorized administrator of UND Scholarly Commons. For more information, please contact zeinebyousif@library.und.edu.

PREPARATION AND CHARACTERIZATION OF MERIDIONALLY TRIS-
CHELATED RHENIUM(I) TERPYRIDINE DICARBONYL COMPLEXES

by

Daniel Ray Black

Bachelor of Science, University of West Georgia, 2008

A Thesis

Submitted to the Graduate Faculty

of the

University of North Dakota

In partial fulfillment of the requirements

for the degree of

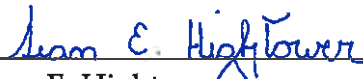
Master of Science

Grand Forks, North Dakota


May

2013


This thesis, submitted by Daniel Ray Black in partial fulfillment of the requirements for the Degree of Master of Science from the University of North Dakota, has been read by the Faculty Advisory Committee under whom the work has been done, and is hereby approved.



Sean E. Hightower
Chairperson




Harmon B. Abrahamson
Committee Member

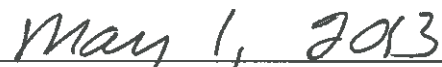


Lothar Stahl
Committee Member

This thesis is being submitted by the appointed advisory committee as having met all of the requirements of the Graduate School at the University of North Dakota and is hereby approved.



Wayne Swisher
Dean of the Graduate School



May 1, 2013

PERMISSION

Title Preparation and Characterization of Meridionally Tris-Chelated
 Rhenium(I) Terpyridine Dicarboxyl Complexes
Department Chemistry
Degree Master of Science

In presenting this thesis in partial fulfillment of the requirements for a graduate degree from the University of North Dakota, I agree that the library of this University shall make it freely available for inspection. I further agree that permission for extensive copying for scholarly purposes may be granted by the professor who supervised my thesis work or, in his absence, by the Chairperson of the department or the dean of the Graduate School. It is understood that any copying or publication or other use of this thesis or part thereof for financial gain shall not be allowed without my written permission. It is also understood that due recognition shall be given to me and to the University of North Dakota in any scholarly use which may be made of any material in my thesis.

Daniel Ray Black
May 6, 2013

TABLE OF CONTENTS

LIST OF FIGURES.....	vi
LIST OF TABLES.....	ix
ACKNOWLEDGMENTS.....	x
ABSTRACT.....	xi
CHAPTER	
I. BACKGROUND.....	1
1.1 Terpyridine Metal Complexes	1
1.2 Rhenium(I) Carbonyl Complexes.....	2
1.3 Problems Related to Bis-Chelating Rhenium(I) Terpyridine Complexes.....	3
1.4 Tris-Chelating Rhenium Terpyridine Complexes.....	4
II. PREPARATION AND CHARACTERIZATION OF RE(TPY-K ³ N)(CO) ₂ L COMPLEXES.....	6
2.1 Materials.....	6
2.2 Measurements.....	7
2.3 Synthesis.....	8
III. RESULTS AND DISCUSSION OF RE(TPY-K ³ N)(CO) ₂ L COMPLEXES.....	19
3.1 Synthetic Preparation	19
3.2 Infrared Spectroscopy.....	21
3.3 Absorption Spectroscopy.....	24
3.4 Nuclear Magnetic Resonance Spectroscopy.....	26
3.5 Mass Spectrometry.....	28
3.6 Electrochemistry.....	29

3.7 Summary.....	34
APPENDICES.....	35
REFERENCES.....	47

LIST OF FIGURES

Figure	Page
1. Structures of 2,2' bipyridine (left) and 2,2'-6',2'' terpyridine (right) with lines of symmetry.....	2
2. Top view of $fac-[Re^I(bpy)(CO)_3(L)]^n$ (left) $fac-[Re^I(tpy-\kappa^2N)(CO)_3(L)]^n$ (right) where L is a negative or where L is a negative or neutral donor ligand such a Cl^- or PPh_3 and n is 0 or +1.....	3
3. Synthesis of meridionally-coordinated tridentate terpyridine rhenium dicarbonyl complexes, $mer,cis-Re[(tpy-\kappa^3N)(CO)_2(L)]^n$. (Reagents and Conditions: (i) 1.1 eq. terpyridine, toluene, reflux 4–8 hrs., (ii) 275°C, 4–6 hrs., (iii) 1.1 eq. $Ag(CF_3SO_3)$, CH_3CN , reflux 5 hrs., (iv) excess of L, THF, reflux 2–6 hrs., (v) 1.1 eq. $Ag(CF_3SO_3)$, CH_2Cl_2 , reflux 8 hrs., (vi) CH_3CN , reflux 5 hrs. n is 1 ⁺ or 0 depending on ligand. L is complex 2-13.....	21
4. Infrared spectra for selected complexes. $mer,cis-Re(tpy-\kappa^3N)(CO)_2Cl$ (1; black, solid line); $mer,cis-[Re(tpy-\kappa^3N)(CO)_2(PEt_3)]^+$ (7; blue, dash dot), and $mer,cis-[Re(tpy-\kappa^3N)(CO)_2(P(OEt)_3)]^+$ (10; red, short dash).....	22
5. Carbonyl stretching frequencies against Tolman electronic parameter, χ , for the phosphine and phosphite complexes.....	24
6. UV–visible spectra for selected $mer,cis-Re[(tpy-\kappa^3N)(CO)_2(L)]^n$ complexes in acetonitrile at a room temperature. $mer,cis-Re(tpy-\kappa^3N)(CO)_2Cl$ 1; black, solid line); $mer,cis-Re(tpy-\kappa^3N)(CO)_2CN$ (4, green, long dash); $mer,cis-[Re(tpy-\kappa^3N)(CO)_2(PEt_3)]^+$ (7; blue, dash dot), and $mer,cis-[Re(tpy-\kappa^3N)(CO)_2(P(OEt)_3)]^+$ (10; red, short dash).....	25

7. Complex 1 absorption spectra in water, acetonitrile, and dichloromethane.....	26
8. NMR spectra of <i>fac</i> -Re(tpy- κ^2 N)(CO) ₃ Cl (top) and <i>mer,cis</i> -Re(tpy- κ^3 N)(CO) ₂ Cl (bottom) in DMSO- <i>d</i> ₆	28
9. Rhenium dimer corresponding the monoisotopic mass found for complex 4.....	29
10. Cyclic Voltammograms for <i>mer,cis</i> -Re(tpy- κ^3 N)(CO) ₂ Cl (1; bottom) and <i>mer,cis</i> -[Re(tpy- κ^3 N)(CO) ₂ (PEt ₃)] ⁺ (7; top).....	32
11. Infrared Spectra of Complexes 1-13 in the carbonyl region.....	36-38
12. ¹ H NMR of <i>mer,cis</i> -Re(tpy- κ^3 N)(CO) ₂ Cl (1) in DMSO- <i>d</i> ₆	39
13. ¹ H NMR of <i>mer,cis</i> -Re(tpy- κ^3 N)(CO) ₂ (OSO ₂ CF ₃) (2) in DMSO- <i>d</i> ₆	39
14. ¹ H NMR of <i>mer,cis</i> -[Re(tpy- κ^3 N)(CO) ₂ (CH ₃ CN)]CF ₃ SO ₃ (3) in acetonitrile- <i>d</i> ₃	39
15. ¹ H NMR of <i>mer,cis</i> -Re(tpy- κ^3 N)(CO) ₂ (CN)(4) in acetonitrile- <i>d</i> ₃	40
16. ¹ H NMR of <i>mer,cis</i> -[Re(tpy- κ^3 N)(CO) ₂ (NC ₅ H ₅)]CF ₃ SO ₃ (5) in acetonitrile- <i>d</i> ₃	40
17. ¹ H NMR of <i>mer,cis</i> -[Re(tpy- κ^3 N)(CO) ₂ (PMe ₃)]CF ₃ SO ₃ (6) in acetonitrile- <i>d</i> ₃	40
18. ¹ H NMR of <i>mer,cis</i> -[Re(tpy- κ^3 N)(CO) ₂ (PEt ₃)]CF ₃ SO ₃ (7) in acetonitrile- <i>d</i> ₃	41
19. ¹ H NMR of <i>mer,cis</i> -[Re(tpy- κ^3 N)(CO) ₂ (PPh ₃)]CF ₃ SO ₃ (8) in acetonitrile- <i>d</i> ₃	41
20. ¹ H NMR of <i>mer,cis</i> -[Re(tpy- κ^3 N)(CO) ₂ (P(OMe) ₃)]CF ₃ SO ₃ (9) in acetonitrile- <i>d</i> ₃	41

21. ^1H NMR of <i>mer,cis</i> -[Re(tpy- $\kappa^3\text{N}$)(CO) $_2$ (P(OEt) $_3$)]CF $_3$ SO $_3$ (10) in acetonitrile- d_3	41
22. ^1H NMR of <i>mer,cis</i> -[Re(tpy- $\kappa^3\text{N}$)(CO) $_2$ (P(OPh) $_3$)]CF $_3$ SO $_3$ (11) in acetonitrile- d_3	42
23. ^1H NMR of <i>mer,cis</i> -[Re(tpy- $\kappa^3\text{N}$)(CO) $_2$ (P(O ^{<i>i</i>} Pr) $_3$)]CF $_3$ SO $_3$ (12) in acetonitrile- d_3	42
24. ^1H NMR of <i>mer,cis</i> -[Re(tpy- $\kappa^3\text{N}$)(CO) $_2$ (P(OMe)(Ph) $_2$)]CF $_3$ SO $_3$ (13) in acetonitrile- d_3	42
25. Randles-Sevcik plot of <i>mer, cis</i> - Re(tpy- $\kappa^3\text{N}$)(CO) $_2$ Cl with a coefficient of determination value of 0.9969.....	45
26. Randles-Sevcik plot of decamethylferrocene with a coefficient of determination value of 0.9986.....	46

LIST OF TABLES

Table	Page
1. $\nu(\text{CO})$ Frequencies for <i>mer,cis</i> -[Re(tpy- κ^3 N)(CO) ₂ L] (CF ₃ SO ₃) and Electronic Parameters of L	22
2. Summary of Electrochemical Potentials for Complexes 1-13.....	30
3. Peak Current, Scan Rates and Square Root of Scan Rates of <i>mer,cis</i> -Re(tpy- κ^3 N)(CO) ₂ Cl.....	45
4. Peak Current, Scan Rates and Square Root of Scan Rates of Decamethylferrocene.....	46

ACKNOWLEDGMENTS

This thesis is dedicated to my wife, Meagan and my sons, Liam & Matthew for all of their support. I would also like to thank my parents, Leslie and Kari, for the encouragement to keep going.

ABSTRACT

Recent work has uncovered a synthetic route to a new series of meridionally-coordinated tridentate terpyridine rhenium dicarbonyl complexes. The complex *mer,cis*-Re(tpy- κ^3N)(CO)₂Cl (**1**) undergoes facile chloride substitution to produce a variety of complexes of the type *mer,cis*-[Re(tpy- κ^3N)(CO)₂(L)]ⁿ, where L = CF₃SO₃ (**2**), CH₃CN (**3**), CN (**4**), NC₅H₅ (**5**), PMe₃ (**6**), PEt₃ (**7**), PPh₃ (**8**), P(OMe)₃ (**9**), P(OEt)₃ (**10**), P(OPh)₃ (**11**), P(OⁱPr)₃ (**12**), P(OMe)(Ph)₂ (**13**). Complexes **1-13** absorb light throughout a significant portion of the visible spectrum. The electrochemistry of these compounds is discussed in relation to their observed π -acidity and their ability to significantly stabilize the lower oxidation state of rhenium relative to the tricarbonyl bipyridine systems. The complex *mer,cis*-Re(tpy- κ^3N)(CO)₂Cl (**1**) produces a first oxidation potential (reversible) that is 0.85 V (vs. SCE) less oxidizing relative to *fac*-Re(bpy)(CO)₃Cl's first oxidation potential (irreversible).

I. BACKGROUND

1.1 Terpyridine Metal Complexes

Some of the most interesting transition metal complexes in inorganic chemistry show stability as well as desirable photophysics and redox properties. Many of these complexes studied contain polypyridine ligands. For example, $[\text{Ru}(\text{bpy})_3]^{2+}$ (where bpy is 2,2' bipyridine) exhibits a combination of chemical stability and desirable photophysical and redox properties.¹ Recently, terpyridine (tpy) metal complexes have received significant interest in coordination chemistry, material science, biochemistry and supramolecular chemistry.²⁻⁸ Terpyridine and its derivatives have been coordinated to various transition metals with potential applications in solar energy conversion,⁹⁻¹³ photocatalytic water splitting,^{14,15} DNA assembly,¹⁶ carbon-carbon single bond formation,¹⁷ and oxidation of alcohols and ethers.¹⁸ As shown in Figure 1, terpyridine has a two-fold axis through the 4' position. Assuming terpyridine is fully coordinated to a metal, the number of possible isomers when attached to a surface, such as titanium dioxide, will be much fewer when compared to bipyridine metal complexes.^{2,9} Terpyridine also has the ability to chelate in a tridentate fashion to

metal centers whereas bipyridine is limited to bidentate chelation. The additional chelation site contributes to metal terpyridine complexes overall stability.

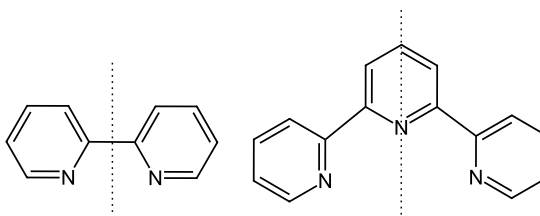


Figure 1. Structures of 2,2' bipyridine (left) and 2,2'-6',2'' terpyridine (right) with two-fold axis included.

1.2 Rhenium(I) carbonyl complexes

Polypyridine complexes containing transition metals such as Ru(II), Os(II), and Re(I) continue to attract considerable attention due to their rich photochemistry and photophysics,²⁰⁻²² their potential applications in the fields for both photocatalysis and electrocatalysis,^{23,24} artificial photosynthetic materials,²⁵⁻²⁷ supramolecular systems,²⁸ photodevices,²⁹⁻³¹ and even cell imaging.^{32,33} Much of this work has been driven by bidentate polypyridine chelates, such as bipyridine or phenanthroline.²¹ Additionally, preparation of rhenium(I) diamine tricarbonyl complexes and subsequent tuning of the electronic properties by modification of different ligands is well known.³⁴⁻³⁹ Even though these complexes have been extensively studied these types of complexes only absorb a small portion of the visible spectrum and have high oxidation potentials. As potential alternative to bipyridine, terpyridine has been studied with rhenium(I) carbonyl systems.

1.3 Problems Related to Bis-Chelating Rhenium(I) Terpyridine Complexes

Complexes of the type $fac-[Re(tpy-\kappa^2N)(CO)_3(L)]^n$ have been prepared (including many terpyridine derivatives) using similar methods to $fac-[Re(bpy)(CO)_3(L)]^n$.⁴⁰⁻⁴⁸ Terpyridine chelates in a bidentate configuration when forming $fac-[Re(tpy-\kappa^2N)(CO)_3(L)]^n$ (where L is a negative or neutral donor ligand such Cl^- or PPh_3 and n is 0 or +1). The $fac-[Re(tpy-\kappa^2N)(CO)_3(L)]^n$ suffers from lack of symmetry similar to $fac-[Re(bpy)(CO)_3(L)]^n$ complexes (see Figure 2). This asymmetry causes isomers when added to a surface such as titanium dioxide.

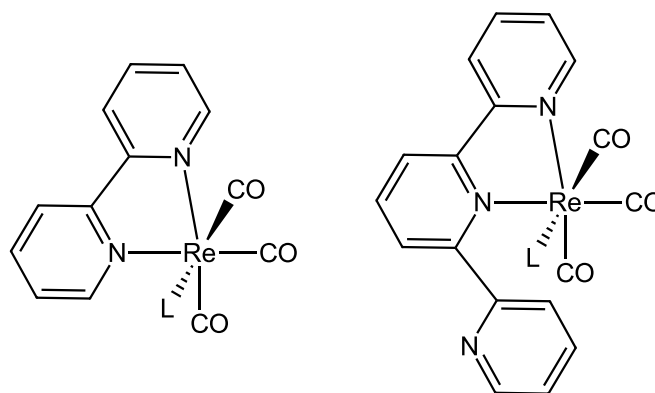


Figure 2. Top view of $fac-[Re(bpy)(CO)_3(L)]^n$ (left) $fac-[Re(tpy-\kappa^2N)(CO)_3(L)]^n$ (right) where L is a negative or neutral donor ligand such a Cl^- or PPh_3 and n is 0 or +1.

Recent research has focused the uncoordinated pyridine ring, $fac-[Re(tpy-\kappa^2N)(CO)_3(L)]^n$ and the mechanism for the Re–N linkage fluxion.^{45,49} Using low temperature NMR, these studies indicate the Re–N linkage movement occurs as a rotation of the ligand using the middle nitrogen coordination as a pivot point. Similar studies have confirmed similar result with terpyridine derivative.⁴⁷⁻⁴⁸

In conjunction with the Re-N linkage fluxion, the uncoordinated nitrogen site of the pyridine from the terpyridine also leads to issues related to reactivity. Amoroso and co-workers demonstrated that the nitrogen on the uncoordinated pyridine ring can be methylated. This methylated nitrogen in turn causes bulkier ligands such as pyridine to be unable to chelate to the rhenium(I) metal center.⁴⁰ To restrict undesirable reactions and improve the complex's symmetry, a tridentate coordinated terpyridine scheme is highly desirable.

1.4. Tris-Chelating Rhenium Terpyridine Complexes

Few rhenium terpyridine complexes with tridentate configurations have been reported. Examples of some of these complexes are

$[\text{Re}^{\text{V}}\text{O}(\text{tpy}-\kappa^3\text{N})(\text{SC}_6\text{H}_4\text{CH}_3)_2]^+$,⁵⁰ $[\text{Re}^{\text{II}}(\text{tpy}-\kappa^3\text{N})(\text{PPh}_3)_2\text{Cl}]^+$,⁵¹ $\text{Re}^{\text{III}}(\text{tpy}-\kappa^3\text{N})\text{Cl}_3$,⁵¹ *mer,cis*- $\text{Re}^{\text{I}}(\text{tpy}-\kappa^3\text{N})(\text{CO})_2\text{Br}$,⁴⁹ $\text{Re}^{\text{II}}\text{Br}(\text{tpy}-\kappa^2\text{N})(\text{PPh}_3)_2$,⁵² and the seven coordinate complex, $[\text{Re}^{\text{III}}(\text{tpy}-\kappa^3\text{N})_2\text{X}]^{2+}$ (where X = Cl, OH, NCS).⁵³ Of the meridionally tris-chelated terpyridine complexes listed, only one rhenium(I) complex has been reported.

Abel and co-workers prepared *mer,cis*- $\text{Re}(\text{tpy}-\kappa^3\text{N})(\text{CO})_2\text{Br}$ complex under harsh conditions using a Carius tube heated to 285 °C.⁴⁹ To date, no studies pertaining to reactivity have been reported for *mer,cis*- $\text{Re}^{\text{I}}(\text{tpy}-\kappa^3\text{N})(\text{CO})_2\text{Br}$. The *mer,cis*- $\text{Re}(\text{tpy}-\kappa^3\text{N})(\text{CO})_2\text{Br}$ was described as a dark brown/black solid which proved to be difficult to dissolve in organic solvents and was characterized by

infrared spectroscopy, proton NMR spectroscopy and elemental analysis . The intense heat and pressure used to prepare the *mer,cis*-Re(tpy- κ^3N)(CO)₂Br denotes excellent thermal stability and the dark brown/black color implies significant absorption in the visible region. Both characteristics are desirable in photocatalysts.

In this study, *mer,cis*-[Re(tpy- κ^3N)(CO)₂L]ⁿ (L = CF₃SO₃ (**2**), CH₃CN (**3**), CN (**4**), NC₅H₅ (**5**), PMe₃ (**6**), PEt₃ (**7**), PPh₃ (**8**), P(OMe)₃ (**9**), P(OEt)₃ (**10**), P(OPh)₃ (**11**), P(OⁱPr)₃ (**12**), P(OMe)(Ph)₂ (**13**) were prepared. Characterization of these complexes using IR spectroscopy, absorption spectroscopy, proton NMR spectroscopy, mass spectrometry and cyclic voltammetry was also performed.

II. PREPARATION AND CHARACTERIZATION OF RE(TPY-K³N)(CO)₂L COMPLEXES

2.1 Materials

Re(CO)₅Cl was purchased from Strem Chemical, Inc. and was used without further purification. The ligands 2,2':6',2''-terpyridine, triphenylphosphine, pyridine, silver trifluoromethanesulfonate, triethyl phosphite, trimethyl phosphite, potassium cyanide, triphenyl phosphite, and triisopropyl phosphite were purchased commercially and used without further purification. The triethylphosphine and trimethylphosphine were purchased from Sigma-Aldrich as 0.1 M solutions in tetrahydrofuran and used without further purification. Re(tpy-κ²N)(CO)₃Cl was prepared from literature.⁴⁰

All solvents for synthesis were of reagent grade and used as received unless otherwise specified. Dry tetrahydrofuran (THF) was distilled from Na-K/benzophenone. For UV-Vis spectroscopy and electrochemical chemical studies HPLC grade or reagent grade was used. The reagent grade acetonitrile was first dried over silica gel (dried for a minimum of 24 hours at 120°C), then filtered removing silica gel and the acetonitrile was distilled over anhydrous calcium hydride.

2.2 Measurements

UV/vis spectra were recorded using a Cary 50 UV-Visible spectrophotometer with a xenon flash lamp. Room temperature emission spectra were measured on a Cary Eclipse fluorescence spectrophotometer. IR spectra were recorded using a thin film technique⁵⁴ with a Perkin-Elmer Spectrum 400 FT-IR/FT-FIR spectrophotometer using 1 cm⁻¹ resolution. The redox potentials of the complexes were measured in an acetonitrile solution containing tetra-*n*-butylammonium hexafluorophosphate (0.1 M) as the supporting electrolyte by cyclic voltammetric techniques using a PINE WaveNow potentiostat analyzer, with a glassy-carbon disk working electrode, a Ag/AgCl, KCl (sat'd) reference electrode, and a Pt counter electrode. The supporting electrolyte was recrystallized in absolute ethanol and dried under vacuum in a dessicator for a minimum of 24 hours prior to use. For the cyclic voltammograms, the potentials were acquired with a Ag⁺/AgCl wire quasi-reference electrode. The voltammograms were corrected using decamethylferrocene (-0.106 V vs. SCE). Decamethylferrocene was chosen as the reference standard because the ferrocene/ferrocenium couple and the first oxidation peak for several of the complexes overlapped. All potentials reported in this paper are versus SCE. ¹H NMR and ³¹P NMR spectra were measured with using a Bruker Avance 500 high-field superconducting NMR spectrometer. Electrospray ionization (ESI) Time of

flight (TOF) mass spectra were obtained with an Agilent Time-of-Flight MS G1969A Series 6200 in positive ionization mode using 1ppm of the complexes in 50% acetonitrile/water (LC/MS) with 10 μ M of acetic acid (ionization agent). Elemental analyses were performed by Atlantic Microlab, Inc., Norcross, GA.

2.3 Synthesis

mer,cis-Re(tpy- κ^3 N)(CO)₂Cl (1). A 35mL heavy-wall, low-expansion borosilicate pressure tube was loaded with *fac-Re(tpy- κ^2 N)(CO)₂Cl*²¹ (71 mg, 0.139 mmol). The tube was then evacuated and purged with an inert gas (such as nitrogen or argon) thrice before being heated to 275 °C for 4-6 hours. A black solid remained. A column of alumina (60 mm length, 30 mm width) was used to purify **1** using dichloromethane, removing any unreacted *fac-Re(tpy- κ^2 N)(CO)₂Cl*, followed by acetonitrile removing a yellow-green product (unidentified). Lastly, ethanol was used to isolate **1**. The resulting solution was removed under reduced pressure leaving **1** as a black solid. Yield: 63 mg, 89%.

Data for 1. ¹H NMR (DMSO-*d*₆): δ 8.87 (d, *J* = 5.6 Hz, 2H), 8.57 (d, *J* = 8.3 Hz, 2H), 8.53 (d, *J* = 8.3 Hz, 2H), 8.21 (t, *J* = 7.9 Hz, 1H), 8.03 (t, *J* = 7.8, 2H), 7.48 (t, *J* = 6.4, 2H). IR (CH₃CN): ν (CO) = 1891, 1798 cm⁻¹. Anal. Calc. for C₁₇H₁₁ClN₃O₂Re: C, 39.96; H, 2.17; N, 8.22 %. Found: C, 38.18; H, 2.08; N, 7.87 %. Electronic absorption (CH₃CN): λ_{\max} , nm (ϵ , M⁻¹cm⁻¹) 239 (29790), 271 (51217), 280 (47492), 317 (25838), 320 (26560), 397 (4042), 460 (3849), 671 (1453). ESI MS: *m/z* 512 (parent

peak, $[M+H]^+$, where M is *mer,cis*-Re(tpy- κ^3 N)(CO)₂Cl), 511 [M], 476 [M-Cl], 397 [M-Cl-pyridine].

***mer,cis*-Re(tpy- κ^3 N)(CO)₂(CF₃SO₃) (2).** A dichloromethane solution (100 mL) containing complex **1** (54 mg, 1.1×10^{-2} mmol) and silver trifluoromethanesulfonate (34 mg, 1.3×10^{-2} mmol) was refluxed under a nitrogen atmosphere for 8 h. After removal of the AgCl precipitate by filtration, the resulting solution was concentrated to a minimum volume under a reduced pressure. Diethyl ether was added drop wise to give a green precipitate. The precipitate was collected by filtration, washed with two 20 mL portions of cold diethyl ether, and dried in vacuo. Yield: 58 mg, 88%.

Data for 2. ¹H NMR (C DMSO-*d*₆): δ 8.96 (d, *J* = 5.3 Hz, 2H), 8.62 (dd, *J* = 15.3, 8.1 Hz, 4H), 8.35 (t, *J* = 8.1 Hz, 1H), 8.16 (t, *J* = 7.9 Hz, 2H), 7.60 (t, *J* = 6.7 Hz, 2H). IR: (CH₂Cl₂): ν (CO) = 1900, 1825 cm⁻¹. λ_{\max} , nm (ϵ , M⁻¹cm⁻¹) 273 (1969), 280 (2267), 318 (3679), 376 (412), 423 (478) 612 (153).

***mer,cis*-[Re(tpy- κ^3 N)(CO)₂(CH₃CN)](CF₃SO₃) (3).** An acetonitrile solution (15 mL) containing complex **2** (49 mg, 7.8×10^{-2} mmol) was refluxed for 5 h under a nitrogen atmosphere. *Alternatively*, **3** was prepared in a one-pot synthesis by refluxing complex **1** (54 mg, 1.1×10^{-2} mmol) and silver trifluoromethanesulfonate (34 mg, 1.3×10^{-2} mmol) in 20 mL of acetonitrile for 8 hours in the dark under nitrogen atmosphere. In either case, the resulting solution was concentrated to ~5

mL under a reduced pressure and diethyl ether was added drop wise to the filtrate to give a green precipitate. The precipitate was collected by filtration, washed with two 20 mL portions of cold diethyl ether, and dried in vacuo. Yield: 47 mg, 90%.

Data for 3. ^1H NMR (CD_3CN): δ 8.91 (d, $J = 5.1$ Hz, 2H), 8.34 (d, $J = 8.5$ Hz, 2H), 8.30 (d, $J = 8.5$ Hz, 2H), 8.20 (t, $J = 8.3$ Hz, 1H), 8.02 (t, $J = 5.2$ Hz, 2H), 7.45 (td, $J = 5.0$ Hz, 2H), 1.97 (d, $J = 3.0$ Hz, 3H). IR (CH_3CN): $\nu(\text{CO}) = 1921, 1848 \text{ cm}^{-1}$. *Anal.* Calc. for $\text{C}_{20}\text{H}_{14}\text{F}_3\text{N}_4\text{O}_5\text{SRe}$: C, 36.09; H, 2.12; N, 8.42 %. Found: C, 35.61; H, 2.14; N, 8.26 %. Electronic absorption (CH_3CN): λ_{max} , nm ($\epsilon, \text{M}^{-1}\text{cm}^{-1}$) 193 (3831), 272 (880), 280 (846), 319 (1285), 425 (209.1) ESI MS: m/z 517 (parent peak, $[\text{M}]^+$, where M is *mer,cis*- $[\text{Re}(\text{tpy}-\kappa^3\text{N})(\text{CO})_2(\text{NCCH}_3)]^+$).

***mer,cis*-Re(tpy- $\kappa^3\text{N}$)(CO) $_2$ CN (4).** A dry THF solution (50 mL) containing complex **3** (58 mg, 8.7×10^{-2} mmol) and potassium cyanide (280 mg, 4.3 mmol) was refluxed for 3 h under a nitrogen atmosphere. The solvent was removed to dryness under a reduced pressure leaving a dark green solid. A column of alumina (60 mm length, 30 mm width) was used to purify **4** using 1:1 dichloromethane/acetonitrile. The resulting solution was concentrated to a minimum volume under reduced pressure producing complex **4** as a dark green solid. The solid was collected by filtration, washed with 20 mL portions of cold diethyl ether, and dried in vacuo. Yield: 29 mg, 66%.

Data for 4. ^1H NMR (CD_3CN): δ 8.60 (m, 2H), 8.02 (m, 3H), 7.90 (m, 4H), 7.21 (m, 2H). IR (CH_3CN): $\nu(\text{CO}) = 1902, 1835 \text{ cm}^{-1}$. *Anal.* Calc. for $\text{C}_{18}\text{H}_{11}\text{N}_4\text{O}_2\text{Re}$: C, 43.11; H, 2.21; N, 11.17 %. Found: C, 43.09; H, 2.14; N, 11.17 %. Electronic absorption (CH_3CN): λ_{max} , nm (ϵ , $\text{M}^{-1}\text{cm}^{-1}$): 222 (31176), 273 (18001), 280 (17325), 317 (29030), 385 (4323), 445 (3576), 661 (1421). ESI MS: m/z 978 (parent peak, see Figure 4 for proposed structure during ESI MS.)

***mer,cis*-[Re(*tpy*- $\kappa^3\text{N}$)(CO) $_2$ (NC $_5$ H $_5$)](CF $_3$ SO $_3$) (5).** A THF solution (50 mL) containing complex **3** (58 mg, 8.7×10^{-2} mmol) and pyridine (0.25 mL, 3.1 mmol) was refluxed for 2 h under a nitrogen atmosphere. The resulting dark green solution was concentrated to a minimum volume under a reduced pressure and diethyl ether was added dropwise to the filtrate to give a green precipitate. The precipitate was collected by filtration, washed with two 20 mL portions of cold diethyl ether, and dried in vacuo. Yield: 53 mg, 87%.

Data for 5. ^1H NMR (CD_3CN): δ 8.99 (d, $J = 5.6$, 2H), 8.32 (d, $J = 8.3$, 2H), 8.28 (d, $J = 8.3$, 2H), 8.17 (t, $J = 8.6$, 1H), 8.01 (m, 4H), 7.77 (m, 1H), 7.48 (m, 2H), 7.21 (m, 2H). IR (CH_3CN): $\nu(\text{CO}) = 1912, 1841 \text{ cm}^{-1}$. *Anal.* Calc. for $\text{C}_{23}\text{H}_{16}\text{F}_3\text{N}_4\text{O}_5\text{SRe}$: C, 39.26; H, 2.29; N, 7.96 %. Found: C, 38.92; H, 2.29; N, 7.45 %. Electronic absorption (CH_3CN): λ_{max} , nm (ϵ , $\text{M}^{-1}\text{cm}^{-1}$): 198 (22216), 249 (6745), 270 (3824), 281 (4129), 322 (6067), 383 (861), 444 (694). ESI MS: m/z 555 (parent peak, $[\text{M}]^+$, where $[\text{M}]^+$ is *mer,cis*-Re(*tpy*- $\kappa^3\text{N}$)(CO) $_2$ (NC $_5$ H $_5$) $^+$).

***mer,cis*-[Re(tpy- κ^3 N)(CO)₂(PMe₃)](CF₃SO₃) (6).** Complex 3 (50 mg, 7.5x10⁻² mmol) was added to dry THF (50 mL) and purged for 10 min. A 0.1 M solution of trimethylphosphine in THF (*ca.* 2.5 mL, 24.0 mmol) was then added to solution and refluxed for 5 hr under a nitrogen atmosphere. The resulting dark green solution was concentrated to a minimum volume under a reduced pressure. Diethyl ether was added drop wise to the filtrate to give a green precipitate. The precipitate was collected by filtration, washed with two 20 mL portions of cold diethyl ether, and dried in vacuo. Yield: 48 mg, 86%.

Data for 6. ¹H NMR (CD₃CN): δ 8.94 (d, *J* = 6.61 Hz, 2H), 8.34 (m, 4H), 8.17 (ddt, *J* = 9.7 Hz, 2H), 7.98 (m, 1H), 7.42 (m, 2H), 1.4 (m, 2H), 0.78 (m, 6H). ³¹P NMR (CDCl₃): δ -31.27 (s, 1P). IR (CH₃CN): ν (CO) = 1918, 1848 cm⁻¹. Anal. Calc. for C₂₁H₂₀F₃N₃O₅PreS: C, 36.00; H, 2.88; N, 6.00 %. Found: C, 35.86; H, 2.79; N, 6.01 %. Electronic absorption (CH₃CN): λ_{\max} , nm (ϵ , M⁻¹cm⁻¹) 229 (3936), 272 (2198), 281 (2271), 318 (4406), 375 (590), 433 (645), 510 (247), 618 (204). ESI MS: *m/z* 552 (parent peak, [M]⁺, where M is *mer,cis*-Re(tpy- κ^3 N)(CO)₂(P(CH₃)₃)⁺).

***mer,cis*-[Re(tpy- κ^3 N)(CO)₂(PEt₃)](CF₃SO₃) (7).** Complex 3 (54 mg, 8.1x10⁻² mmol) was added to dry THF (50 mL) and purged for 10 min. A 0.1 M solution of triethylphosphine in THF (*ca.* 2.5 mL, 26.4 mmol) was then added to solution and refluxed for 5 hr under a nitrogen atmosphere. The resulting dark green solution was concentrated to a minimum volume under a reduced pressure.

Diethyl ether was added drop wise to the filtrate to give a green precipitate. The precipitate was collected by filtration, washed with two 20 mL portions of cold diethyl ether, and dried in vacuo. Yield: 56 mg, 93%.

Data for 7. ^1H NMR (CD_3CN): δ 8.99 (d, J = 5.9 Hz, 2H), 8.36 (d, J = 9.9 Hz, 2H), 8.31 (d, J = 8.9 Hz, 2H), 8.16 (t, J = 8.4 Hz, 1H), 7.98 (t, J = 7.4 Hz, 2H), 7.41 (t, J = 6.4 Hz, 2H), 1.22 (m, 6H) 0.63 (m, 9H). ^{31}P NMR (CDCl_3): δ -12.25 (s, 1P). IR (CH_3CN): $\nu(\text{CO}) = 1927, 1855 \text{ cm}^{-1}$. *Anal. Calc.* for $\text{C}_{24}\text{H}_{26}\text{F}_3\text{N}_3\text{O}_5\text{PReS}$: C, 38.81; H, 3.53; N, 5.66 %. Found: C, 39.01; H, 3.41; N, 5.57 %. Electronic absorption (CH_3CN): λ_{max} , nm (ϵ , $\text{M}^{-1}\text{cm}^{-1}$): 271 (1579), 273 (1583), 322 (1732), 435 (308), 681 (101). ESI MS: m/z 594 (parent peak, $[\text{M}]^+$, where $[\text{M}]^+$ is *mer,cis*- $[\text{Re}(\text{tpy}-\kappa^3\text{N})(\text{CO})_2(\text{P}(\text{Et}_3))]^+$), 566 $[\text{M} - \text{CO}]$, 504 $[\text{M} - \text{C}_2\text{H}_{10}\text{O}_2]$, 475 $[\text{M} - \text{P}(\text{Et}_3)]$.

***mer,cis*- $[\text{Re}(\text{tpy}-\kappa^3\text{N})(\text{CO})_2(\text{PPh}_3)](\text{CF}_3\text{SO}_3)$ (8).** A THF solution (50 mL) containing complex **3** (55 mg, 8.3×10^{-2} mmol) with triphenylphosphine (1.389 g, 5.3 mmol) was refluxed for 4 h under a nitrogen atmosphere. The resulting dark green solution was concentrated to ~5 mL under a reduced pressure and diethyl ether was added drop wise to the filtrate to give a green precipitate. A column of alumina (25 mm length, 30 mm diameter) was used to isolate the product. 100% diethyl ether was used to remove the excess triphenylphosphine followed by acetonitrile (producing a dark green band). The excess eluent was concentrated under a reduced pressure. Cold hexane was added to produce a green

precipitate. The precipitate was collected by filtration, washed with two 20 mL portions of cold diethyl ether, and dried in vacuo. Yield: 69 mg, 94%.

Data for 8. ^1H NMR (CD_3CN): δ 9.04 (d, $J = 5.5$ Hz, 2H), 7.94 (d, $J = 6.5$ Hz, 4H), 7.77 (t, $J = 7.8$ Hz, 2H), 7.35 (t, $J = 6.6$ Hz, 3H), 7.27 (t, $J = 6.5$ Hz, 3H), 7.22 (m, 6H), 7.03 (m, 6H). ^{31}P NMR (CDCl_3): δ 27.32 (s, 1P). IR (CH_3CN): $\nu(\text{CO}) = 1911, 1838$ cm^{-1} . *Anal. Calc.* for $\text{C}_{36}\text{H}_{26}\text{F}_3\text{N}_3\text{O}_5\text{PReS}$: C, 48.76; H, 2.96; N, 4.74 %. Found: C, 48.95; H, 2.95; N, 4.45 %. Electronic absorption (CH_3CN): λ_{max} , nm (ϵ , $\text{M}^{-1}\text{cm}^{-1}$): 255 (7443), 322 (31134), 377 (942), 435 (863), 610 (290). ESI MS: m/z 738 (parent peak, $[\text{M}]^+$, where M is *mer,cis-Re^I(tpy- κ^3 N)(CO)₂(PPh₃)⁺*).

mer,cis-[Re(tpy- κ^3 N)(CO)₂(P(OMe)₃)](CF₃SO₃) (9). Complex **9** was prepared by refluxing complex **3** (49 mg, 7.4×10^{-2} mmol) and trimethyl phosphite (2.5 mL, 21.2 mmol) in dry THF (50 mL) under nitrogen atmosphere for 2 hours. The dark green solution was concentrated to a minimum volume under a reduced pressure. Pentane was added dropwise to the concentrate giving a green solid. The green precipitate was filtered and washed with five 10 mL portions of cold diethyl ether. The solid was dried in vacuo. Yield: 51 mg, 88%.

Data for 9. ^1H NMR (CD_3CN): δ 8.97 (d, $J = 8.9$ Hz, 2H), 8.33 (m, 4H), 8.19 (ddd, $J = 8.4$ Hz, 2H), 8.00 (m, 1H), 7.41 (m, 2H), 3.26 (d, $J = 10.68$ Hz, 9H). ^{31}P NMR (CDCl_3): δ 109.03 (s, 1P). IR (CH_3CN): $\nu(\text{CO}) = 1940, 1863$ cm^{-1} . *Anal. Calc.* for $\text{C}_{21}\text{H}_{20}\text{F}_3\text{N}_3\text{O}_8\text{PReS}$: C, 33.69; H, 2.69; N, 5.61 %. Found: C, 33.46; H, 2.73; N,

5.62 %. Electronic absorption (CH₃CN): λ_{\max} , nm (ϵ , M⁻¹cm⁻¹) 228 (32564), 272 (19335), 279 (19855), 314 (34778), 367 (3736), 408 (4411), 600 (1022). ESI MS: m/z 600 (parent peak, [M]⁺, where M is *mer,cis*-Re(tpy- κ^3 N)(CO)₂(P(OCH₃)₃)⁺).

***mer,cis*-[Re(tpy- κ^3 N)(CO)₂(P(OEt)₃)](CF₃SO₃) (10).** Complex **10** was prepared by refluxing complex **3** (45 mg, 6.8 × 10⁻² mmol) and triethyl phosphite (*ca.* 0.35 mL, 2.0 mmol) in THF (50 mL) under a nitrogen atmosphere for 2 hours. The dark green solution was concentrated to a minimum volume under a reduced pressure. Diethyl ether was added dropwise to the concentrate giving a green solid. The green precipitate was filtered and washed with five 10 mL portions of cold diethyl ether. The solid was dried in vacuo. Yield: 51 mg, 88%.

Data for 10. ¹H NMR (CD₃CN): δ 8.96 (d, J = 9.0 Hz, 2H), 8.35 (d, J = 8.1 Hz, 2H), 8.30 (dt, J = 10.2 Hz, 2H), 8.17. (m, 1H), 7.98 (m, 2H), 7.40 (m, 2H), 3.63 (p, J = 27.5 Hz, 6H), 0.84 (t, J = 14.0 Hz, 9H). ³¹P NMR (CD₃CN): δ 105.27 (s, 1P). IR (CH₃CN): ν (CO) = 1938, 1863 cm⁻¹. Anal. Calc. for C₂₄H₂₆F₃N₃O₈PREs: C, 36.46; H, 3.31; N, 5.31 %. Found: C, 36.37; H, 3.33; N, 5.32 %. Electronic absorption (CH₃CN), λ_{\max} , nm (ϵ , M⁻¹cm⁻¹): 229 (33186), 272 (18922), 280 (20013), 314 (38358), 367 (3876), 411 (4781), 481 (1679), 530 (1546), 576 (1362). ESI MS: m/z 642 (parent peak, [M]⁺, where M is *mer,cis*-Re(tpy- κ^3 N)(CO)₂(P(OEt)₃)⁺).

***mer,cis*-[Re(tpy- κ^3 N)(CO)₂(P(OPh)₃)](CF₃SO₃) (11).** Complex **11** was prepared by refluxing complex **3** (39 mg, 5.9 × 10⁻² mmol) and triphenyl phosphite (*ca.* 0.46

mL, 1.8 mmol) in dry THF (50 mL) under nitrogen atmosphere for 2 hours. The dark green solution was concentrated to a minimum volume under a reduced pressure. Diethyl ether was added dropwise to the concentrate giving a green solid. The green precipitate was filtered and washed with five 10 mL portion of cold diethyl ether. The solid was dry under vacuo. Yield: 53 mg, 96%.

Data for 11. ^1H NMR (CD_3CN): δ 8.47 (m, 2H), 8.20 (m, 3H), 8.09 (ddd, $J = 8.7, 7.6, 1.2$ Hz, 1H), 7.92 (td, $J = 7.8, 1.6$ Hz, 2H), 7.38 (tt, $J = 7.6, 2.3$ Hz, 2H), 7.17 (m, 12H), 6.76 (m, $J = 27.5$ Hz, 5H). ^{31}P NMR (CDCl_3): δ 92.87 (s, 1P). IR (CH_3CN): ν (CO) = 1952, 1874 cm^{-1} . *Anal.* Calc. for $\text{C}_{35}\text{H}_{26}\text{F}_3\text{N}_3\text{O}_8\text{PReS}$: C, 46.25; H, 2.80; N, 4.49 %. Found: C, 46.32; H, 2.83; N, 4.42 %. Electronic absorption (CH_3CN): λ_{max} , nm (ϵ , $\text{M}^{-1}\text{cm}^{-1}$): 243 (35770), 274 (22843), 282 (22220), 313 (36302), 403 (5018), 465 (1585), 504 (1460). ESI MS: m/z 786 (parent peak, $[\text{M}]^+$, where M is *mer,cis*- $\text{Re}(\text{tpy-}\kappa^3\text{N})(\text{CO})_2(\text{P}(\text{OPh})_3)]^+$).

***mer,cis*-[$\text{Re}(\text{tpy-}\kappa^3\text{N})(\text{CO})_2(\text{P}(\text{O}^i\text{Pr})_3)](\text{CF}_3\text{SO}_3)$ (12).** Complex 12 was prepared by refluxing complex 3 (32 mg, 4.8×10^{-2} mmol) and triethyl phosphite (ca. 0.36 mL, 2.0 mmol) in dry THF (50 mL) under nitrogen atmosphere for 2 hours. The dark green solution was concentrated to a minimum volume under a reduced pressure. Diethyl ether was added dropwise to the concentrate giving a green solid. The green precipitate was filtered and washed with five 10 mL portions of cold diethyl ether. The solid was dried in vacuo. Yield: 36 mg, 90%.

Data for 12. ^1H NMR (CD_3CN): δ 8.97 (ddt, $J = 5.6, 1.6, 0.8$ Hz, 2H), 8.32 (m, 4H), 8.17 (m, 1H), 7.97 (tdd, $J = 8.3, 1.5, 0.7$ Hz, 2H), 7.41 (ddd, $J = 7.6, 5.6, 1.4$ Hz, 2H), 4.36 (dp, $J = 8.4, 6.1$ Hz, 3H), 0.85 (d, $J = 6.1$ Hz, 27H). ^{31}P NMR (CDCl_3): δ 103.64 (s, 1P). IR (CH_3CN): $\nu(\text{CO}) = 1935, 1861$ cm^{-1} . *Anal.* Calc. for $\text{C}_{27}\text{H}_{32}\text{F}_3\text{N}_3\text{O}_8\text{ReS}$: C, 38.94; H, 3.87; N, 5.05 %. Found: C, 38.97; H, 3.81; N, 5.09 %. Electronic absorption (CH_3CN): λ_{max} , nm (ϵ , $\text{M}^{-1}\text{cm}^{-1}$): 229 (33818), 272 (18935), 280 (20007), 315 (39587), 368 (4177), 388 (3923), 413 (4803), 584 (4803). ESI MS: m/z 684 (parent peak, $[\text{M}]^+$, where M is *mer,cis*- $\text{Re}(\text{tpy}-\kappa^3\text{N})(\text{CO})_2(\text{P}(\text{OC}_2\text{H}_5)_3)^+$).

***mer,cis*-[$\text{Re}(\text{tpy}-\kappa^3\text{N})(\text{CO})_2(\text{P}(\text{OMe})(\text{Ph})_2)](\text{CF}_3\text{SO}_3)$ (13).** Complex 13 was prepared by refluxing complex 3 (33 mg, 5.0×10^{-2} mmol) and triethyl phosphite (ca. 0.30 mL, 1.5 mmol) in dry THF (50 mL) under a nitrogen atmosphere for 2 hours. The dark green solution was concentrated to a minimum volume under a reduced pressure. Diethyl ether was added dropwise to the concentrate giving a green solid. The green precipitate was filtered and washed with five 10 mL portions of cold diethyl ether. The solid was dried in vacuo. Yield: 39 mg, 93%.

Data for 13. ^1H NMR (CD_3CN): δ 8.98 (dt, $J = 6.1, 1.5$ Hz, 2H), 8.04 (m, 5H), 7.89 (td, $J = 7.9, 1.6$ Hz, 2H), 7.44 (m, 2H), 7.36 (ddd, $J = 7.3, 5.6, 1.5$ Hz, 2H), 7.28 (tt, $J = 6.3, 2.1$ Hz, 4H), 6.98 (ddt, $J = 9.7, 6.7, 1.4$ Hz, 4H), 3.04 (d, $J = 11.5$ Hz, 3H). ^{31}P NMR (CDCl_3): δ 110.58 (s, 1P). IR (CH_3CN): $\nu(\text{CO}) = 1931, 1858$ cm^{-1} . *Anal.* Calc. for $\text{C}_{31}\text{H}_{24}\text{F}_3\text{N}_3\text{O}_6\text{PReS}$: C, 44.28; H, 2.88; N, 5.00 %. Found: C, 44.32; H, 2.85;

N, 4.96 %. Electronic absorption (CH₃CN): λ_{\max} , nm (ϵ , M⁻¹cm⁻¹): 273 (22237), 317 (34238), 364 (4057), 419 (4356), 486 (1535.3), 612 (1088). ESI MS: m/z 692 (parent peak, [M]⁺, where M is *mer,cis*-[Re(tpy- κ^3 N)(CO)₂(P(OC₂H₅)₃)]⁺).

III. RESULTS AND DISCUSSION OF RE(TPY-K³N)(CO)₂L COMPLEXES

3.1 Synthetic Preparation

An outline of the synthesis of the meridionally-coordinated terpyridine rhenium dicarbonyl complexes is given in Figure 3. The preparation of these rhenium dicarbonyl complexes begins with the *fac*-Re(tpy-κ²N)(CO)₃Cl (**1**) complex.⁴⁰ Methods to prepare this complex, as well as other similar bidentate *fac*-Re(α,α'-diimine)(CO)₃Cl complexes, are well-established. Preparation of the meridionally-coordinated tridentate *mer,cis*-Re(tpy-κ³N)(CO)₂Cl (**1**) complex was performed by the thermal elimination of CO via modification to a previous literature report.⁴⁹ Indeed, the initial report detailed the preparation for the similar *mer,cis*-Re(tpy-κ³N)(CO)₂Br from the *fac*-Re(tpy-κ²N)(CO)₃Br complex using a Carius tube. We found this method to be problematic and inconvenient for preparative studies given the difficulties associated with flame sealing the tube under high vacuum. In addition, the possibility of explosion due to over-pressure and product recovery further complicated the process. We found that the use of a heavy-wall, low-expansion borosilicate pressure tube in conjunction with an automatic pressure release and reseal mechanism⁵⁵ greatly simplifies the procedure. Product recovery is vastly simplified, the reaction vessel is reusable,

and the hazards associated with possible explosion due to over-pressure are greatly reduced.

The *mer,cis*-Re(tpy- κ^3N)(CO)₂Cl (**1**) was stable and was used in subsequent reactions for preparing the dicarbonyl complexes. The removal of chloride from the *mer,cis*-Re(tpy- κ^3N)(CO)₂Cl (**1**) was effected by use of silver triflate, Ag(CF₃SO₃), in methylene chloride, yielding *mer,cis*-Re(tpy- κ^3N)(CO)₂(CF₃SO₃) (**2**). Refluxing this complex in acetonitrile produced *mer,cis*-[Re(tpy- κ^3N)(CO)₂(NCCH₃)]⁺ (**3**). Subsequently, the *mer,cis*-[Re(tpy- κ^3N)(CO)₂(NCCH₃)]⁺ (**3**) was prepared directly from *mer,cis*-Re(tpy- κ^3N)(CO)₂Cl (**1**) using Ag(CF₃SO₃) in refluxing acetonitrile. Refluxing *mer,cis*-[Re(tpy- κ^3N)(CO)₂(NCCH₃)]⁺ (**3**) in tetrahydrofuran (THF) with a large excess of the ligand L (L = CN⁻ (**4**), NC₅H₅ (**5**), PMe₃ (**6**), PEt₃ (**7**), PPh₃ (**8**), P(OMe)₃ (**9**), P(OEt)₃ (**10**), P(OPh)₃ (**11**), P(OⁱPr)₃ (**12**), P(OMe)(Ph)₂ (**13**)) resulted in the displacement of acetonitrile and the subsequent coordination of L.

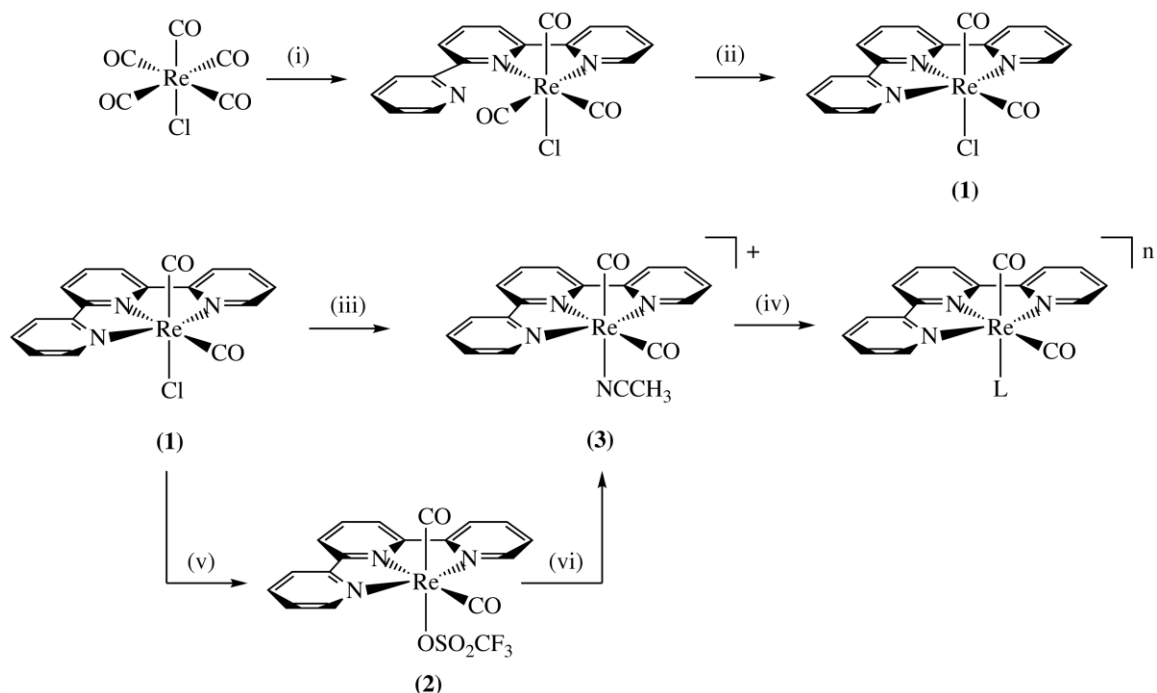


Figure 3. Synthesis of meridionally-coordinated tridentate terpyridine rhenium dicarbonyl complexes, *mer,cis*-Re[(tpy-*k*³N)(CO)₂(L)]ⁿ. (Reagents and Conditions: (i) 1.1 eq. terpyridine, toluene, reflux 4–8 hrs., (ii) 275°C, 4–6 hrs., (iii) 1.1 eq. Ag(CF₃SO₃), CH₃CN, reflux 5 hrs., (iv) excess of L, THF, reflux 2–6 hrs., (v) 1.1 eq. Ag(CF₃SO₃), CH₂Cl₂, reflux 8 hrs., (vi) CH₃CN, reflux 5 hrs. n is 1⁺ or 0 depending on ligand. L is complex 2-13

3.2 Infrared Spectroscopy

The spectrum of the complexes **1**, **7**, and **10** are shown in Figure 4 representative examples showing two vibrational bands were found for all complexes in the region of ca. 1795–1865 and 1890–1940 cm⁻¹ (Appendix A shows the IR spectra in the carbonyl region for complexes **1-13**). The two CO vibrations were expected on the basis of those found for other reported rhenium(I) dicarbonyl complexes;^{56,57} this is consistent with a mutual *cis*-CO geometry for all of the compounds.

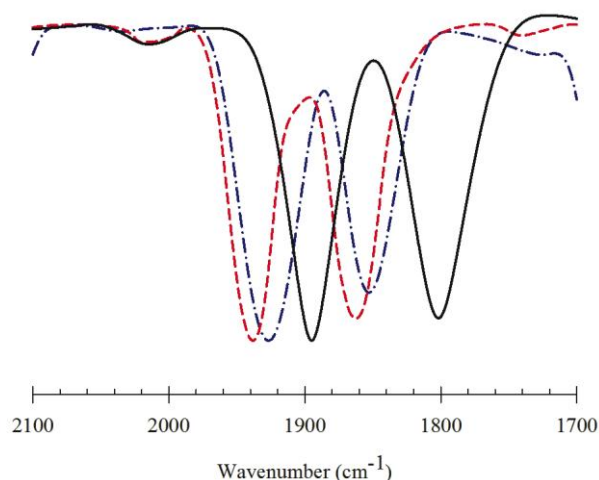


Figure 4. Infrared spectra for selected complexes. *mer,cis*-Re(tpy- κ^3N)(CO)₂Cl (**1**; **black, solid line**); *mer,cis*-[Re(tpy- κ^3N)(CO)₂(PEt₃)⁺ (**7**; **blue, dashdot**), and *mer,cis*-[Re(tpy- κ^3N)(CO)₂(P(OEt)₃)⁺ (**10**; **red, short dash**).

Table 1. $\nu(\text{CO})$ Frequencies for *mer,cis*-[Re(tpy- κ^3N)(CO)₂L] (CF₃SO₃) and Electronic Parameters of L

No.	L	$\nu(\text{CO})$ (cm ⁻¹)	χ^a
6	PMe ₃	1919, 1848	8.55
7	PEt ₃	1927, 1853	6.30
8	PPh ₃	1928, 1855	13.25
9	P(OMe) ₃	1942, 1863	24.10
10	P(OEt) ₃	1938, 1863	21.60
11	P(OPh) ₃	1952, 1874	30.20
12	P(O ⁱ Pr) ₃	1935, 1861	19.05
13	P(OMe)(Ph) ₂	1931, 1858	16.30

^a Taken from ref 58 and χ is the Tolman's Electronic Parameter.

It is well documented that metal carbonyl stretching frequencies are influenced by other coordinated ligands' ability to accept and donate electronic density to and from the metal center.⁵⁹ Tolman's electronic parameter χ measures the electron withdrawing ability of a ligand based on carbonyl stretching frequency of Ni(CO)₃L (where L is a phosphine).⁶⁰ Table 1 lists the Tolman

electronic parameters of the phosphite and phosphine ligands coordinated to the *mer,cis*-[Re(tpy- κ^3N)(CO)₂] moiety with the corresponding carbonyl stretching frequency. Figure 5 show a direct correlation between Tolman electronic values and the carbonyl stretching frequency for complexes **5** - **13**. As ligand L in the *mer,cis*-[Re(tpy- κ^3N)(CO)₂L]⁺ withdraws electron density from the Re^I metal center, the electron density between the Re^I metal center and the carbonyl ligands decreases. The simple explanation is the higher the carbonyl stretching frequency the greater electron withdrawing ability of ligand L for *mer,cis*-[Re(tpy- κ^3N)(CO)₂L]⁺. Extrapolating this relationship to include the non-phosphorus ligands the follow trend can be developed from the greatest electron-acceptor to the lowest electron-acceptor ligand: P(OPh)₃, P(OMe)₃, P(OEt)₃, P(O^{*i*}Pr)₃, P(OMe)Ph₂, PPh₃, PEt₃, PMe₃, NCCH₃, NC₅H₅, CN⁻, OSO₂CF₃⁻, Cl⁻.

Plot of two $\nu(\text{CO})$ frequencies against χ

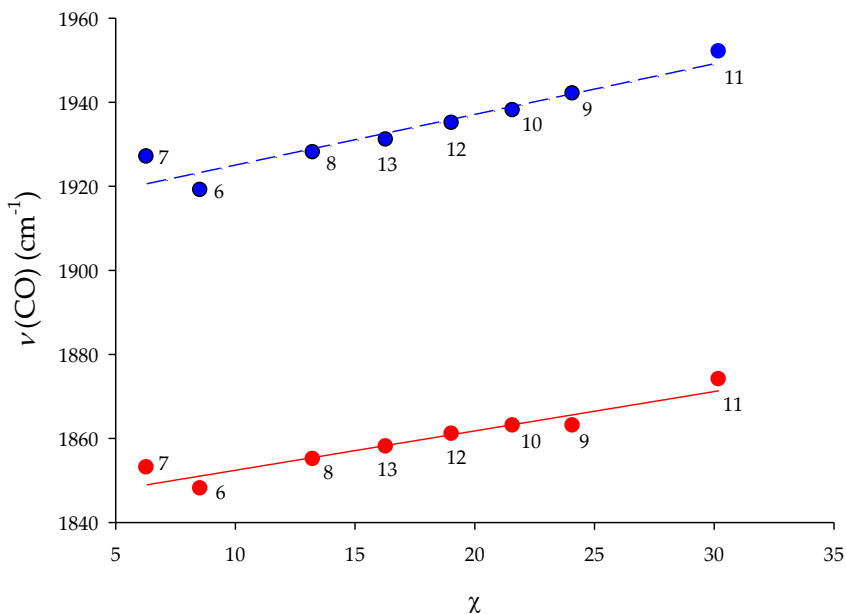


Figure 5. Carbonyl stretching frequencies against Tolman electronic parameter, χ , for the phosphine and phosphite complexes.

3.3 Absorption Spectroscopy

The UV-vis spectra for these complexes were acquired in acetonitrile.

Figure 6 shows the UV-vis spectra for selected complexes plotted as a function of molar extinction coefficients versus wavelength. This allows a direct comparison of transition energies, as well as a measure of the oscillator strengths. All complexes absorb light throughout a significant portion of the visible spectrum. Several of these complexes, the *mer,cis*- $\text{Re}(\text{tpy-}\kappa^3\text{N})(\text{CO})_2\text{Cl}$ (**1**) and *mer,cis*- $\text{Re}(\text{tpy-}\kappa^3\text{N})(\text{CO})_2\text{CN}$ (**4**), absorb light throughout the entire visible spectrum. In the region between 350 and 800 nm, all compounds show at least three broad bands (see inset on Figure 6). The two bands at higher energies are better

resolved with more defined structure relative to the lower energy band. Within this region, the molar extinction coefficients for the chloro, cyano and trialkylphosphite complexes exhibit markedly larger values indicative of increased oscillator strengths. All compounds listed exhibit absorptions between 200 and 325 nm that are assigned to $\pi-\pi^*$ ligand centered transitions, based on previous work for rhenium-terpyridine complexes.⁶¹ Absorptions in the visible region are assigned to metal-to-ligand transitions (MLCT).

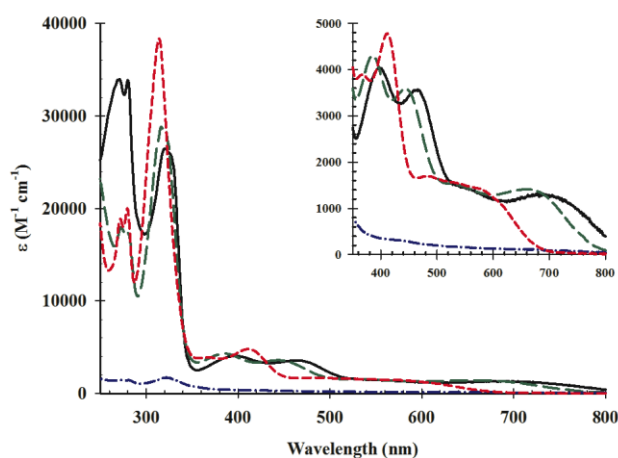


Figure 6. UV-visible spectra for selected *mer,cis*-Re[(tpy- κ^3 N)(CO)₂(L)]ⁿ complexes in acetonitrile at a room temperature. *mer,cis*-Re(tpy- κ^3 N)(CO)₂Cl (**1**; **black, solid line**); *mer,cis*-Re(tpy- κ^3 N)(CO)₂CN (**4**, **green, long dash**); *mer,cis*-[Re(tpy- κ^3 N)(CO)₂(PEt₃)]⁺ (**7**; **blue, dash dot**), and *mer,cis*-[Re(tpy- κ^3 N)(CO)₂(P(OEt)₃)]⁺ (**10**; **red, short dash**).

In addition to the use of acetonitrile, the UV-vis spectrum for Re(tpy- κ^3 N)(CO)₂Cl was acquired in methylene chloride and water to illustrate the solvent sensitivity of the absorption bands in the region from 350 – 800 nm. For example, Figure 7 shows in methylene chloride, a less polar solvent compared to

acetonitrile, leads to a bathochromic shift but with the water a hypsochromic shift is observed, as expected of the MLCT band. In addition, the molar extinction coefficients and the broad peak-widths are consistent with this assignment.

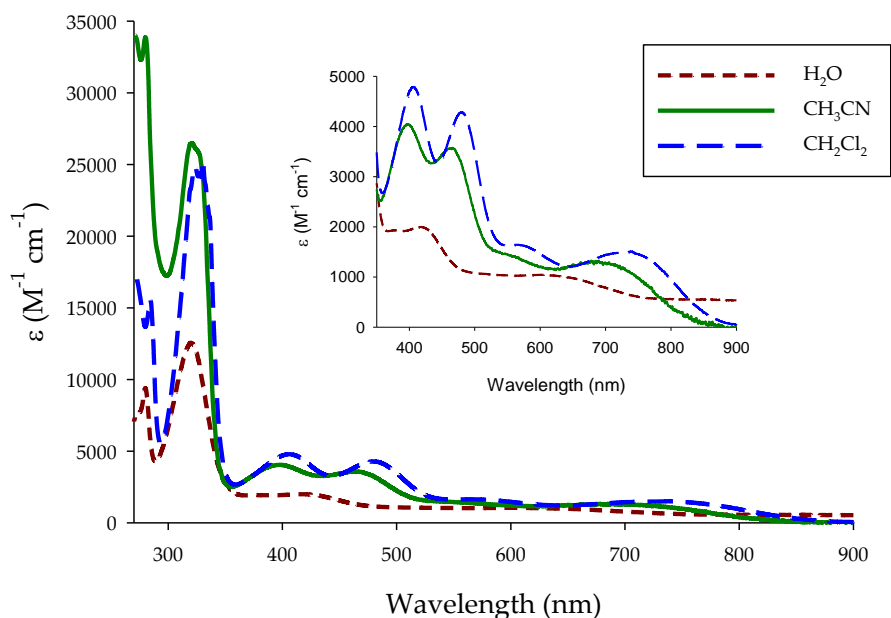


Figure 7. Complex 1 absorption spectra in water, acetonitrile, and dichloromethane.

3.4 Nuclear Magnetic Resonance Spectroscopy

The ^1H NMR spectra were obtained in CD_3CN excluding complex 1 which was obtained in $\text{DMSO}-d_6$ (Appendix A contains ^1H spectra for all complexes). Complex 1 lacked sufficient signal for a quantitative ^1H spectrum using CD_3CN and CD_2Cl_2 . It should also be note that ^{13}C spectra were not obtained. The NMR spectra of complex 1 showed eleven protons in the aromatic region which is

consistent with the eleven protons on terpyridine. When the 2,2':6',2''-terpyridine was initially coordinated to rhenium, as *fac*-Re(tpy- κ^2N)(CO)₃Cl, eleven protons were found to be independent of one another, which implies asymmetry in the complex (see top spectrum in Figure 8). The coordination of the free pyridine ring on the 2,2':6',2''-terpyridine formed the *mer,cis*-Re(tpy- κ^3N)(CO)₂Cl, giving a far more symmetrical complex than *fac*-Re(tpy- κ^2N)(CO)₃Cl. Also a downfield shift was observed for the *mer,cis*-Re(tpy- κ^3N)(CO)₂Cl when compared to *fac*-Re(tpy- κ^2N)(CO)₃Cl. The replacement of Cl⁻ with the various ligands listed here showed no significant shift and a no definite trend could be established (See

Appendix B).

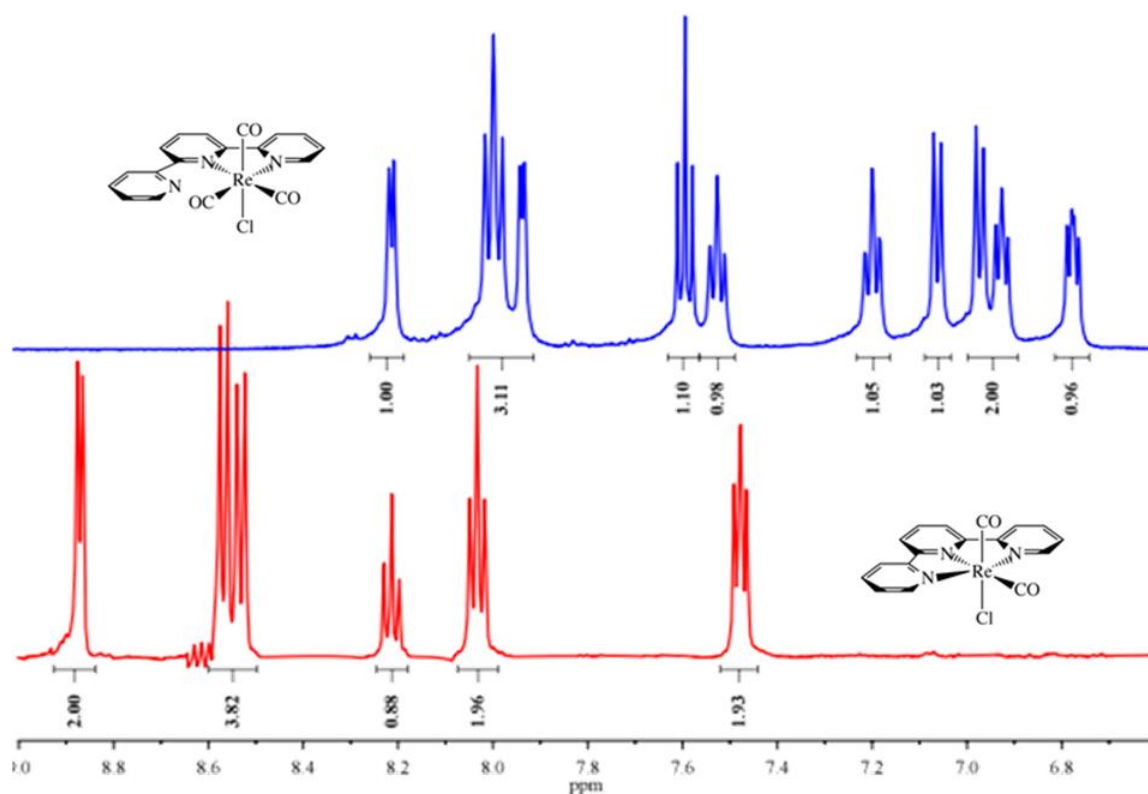


Figure 8. NMR spectra of *fac*-Re(tpy- κ^2 N)(CO)₃Cl (top) and *mer,cis*-Re(tpy- κ^3 N)(CO)₂Cl (bottom) in DMSO-*d*₆.

3.5 Mass Spectrometry

All parent peaks for positively charged complexes were found to be consistent with the calculated values of formulated masses, minus the triflate counter ion. The parent peak of complex **1** was protonated. Interestingly the parent peak of complex **4** was found to have a value of 978.084, which corresponds to a bridged complex depicted in Figure 9.

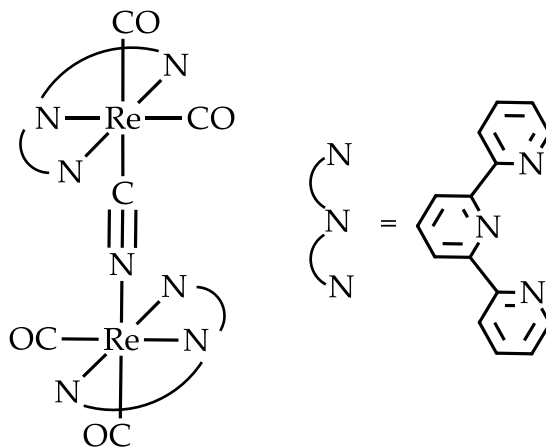


Figure 9. Rhenium dimer corresponding to the monoisotopic mass found for complex 4. The complex in Figure 9 with a monoisotopic mass of 978.083 corresponds well with the experimental value found for complex 4. The bridging of complex 4 is likely caused by the ambidentate nature of the cyanide ligand and is induced by the ionization of mass spectrometric processes. Either the cyano or one of the carbonyl ligands could be the bridging ligand but the cyano ligand is likely to be the bridging ligand; this bridging was not observed in any of the other complexes' mass spectrometric data. Dimer formation in *fac*-Re(bpy- κ^2N)(CO)₃ moieties when using cyanide has been seen in literature.^{62,63}

3.6 Electrochemistry

The electrochemistry of these compounds has been investigated in acetonitrile and the corresponding electrochemical potentials are reported in Table 2.

Table 2. Summary of Electrochemical Potentials for Complexes **1-13**.

No.	L	$E_{1/2}$ (V vs. SCE) ^{a,b}	
		Oxidation	Reduction
1	Cl ⁻	0.48, 0.99 ^c	-1.27, -1.73 ^c
3	NCCH ₃	0.80, 1.59	-1.21 ^c
4	CN ⁻	0.67 ^c , 0.85 ^c	-0.90, -2.12 ^c
5	NC ₅ H ₅	0.86 ^c , 1.35	-1.21 ^c
6	PMe ₃	0.84, 1.21 ^c	-1.21 (65), -1.64 ^c
7	PEt ₃	0.84, 1.22 ^c	-1.21 (65), -1.64 ^c
8	PPh ₃	0.94, 1.31 ^c	-1.19
9	P(OMe) ₃	0.92	-1.24, -1.50 ^c
10	P(OEt) ₃	0.93	-1.23, -1.51 ^c
11	P(OPh) ₃	1.07	-1.21 ^c , -1.41 ^c
12	P(O ⁱ Pr) ₃	0.92	-1.24, 1.58 ^c
13	P(OMe)(Ph) ₂	0.92	-1.23, 1.53 ^c

^a Glassy-carbon disk working (3 mm i.d.) and Pt-wire counter electrodes were used.

^b Scan rate 0.1 V s⁻¹. ^c Irreversible peak.

It is useful to draw comparisons from facial tricarbonyl bipyridine rhenium-types of complexes in interpreting the redox properties for the cis-dicarbonyl meridionally-coordinated terpyridine rhenium systems. For example, the electrochemical behavior for *fac*-Re(α,α' -diimine)(CO)₃Cl complexes has been well-established and was beautifully summarized by Fujita and Brunschwig.⁶⁵ The negative potential region often shows several reduction waves. The first reduction is reversible and is assigned to a ligand-based reduction. The second reduction is usually irreversible and is assigned to a metal-based reduction. The first oxidation is generally observed to be irreversible⁶⁵ and assigned to a metal-based process. This oxidation is followed by the rapid loss of carbon monoxide

due to the weakening of the Re π -backbonding to CO. For the *fac*-Re(bpy)(CO)₃Cl complex under similar experimental conditions employed for this work, the oxidation and reduction potentials are +1.32 V and -1.35 V, respectively. For the *mer,cis*-Re(tpy- κ^3N)(CO)₂Cl (**1**) a one-electron, reversible oxidation is observed at +0.48 V (see Appendix C) which is assigned as metal-based oxidation (*i.e.*, Re^I / Re^{II} oxidation). This is followed by an irreversible oxidation at +1.26 V. Based on the relative invariance of this potential compared to the *fac*-Re(bipyridine)(CO)₃Cl complex, this second oxidation is assigned as the loss of carbon monoxide via a second metal-based oxidation (*i.e.*, Re^{II} / Re^{III} oxidation). A single, quasi-reversible multi-electron reduction wave in the cathodic direction is observed at -1.27 V with the return anodic sweep resulting in two peaks at -1.31 V and -1.16 V. As can be seen from Table 2, this reduction potential is relatively invariant over the series of complexes. Thus, we attribute this potential to ligand-centered (terpyridine) reduction. A second irreversible wave at -1.73 V (not shown in Figure 8) is observed which gives rise to a new set of redox waves. Presumably, this is a metal-based reduction, followed by the rapid loss of Cl⁻. The first oxidation peak, in most cases, is chemically irreversible at scan rates of 0.1–0.2 V·s⁻¹; however, at much faster sweep rates a reversible wave is observed.

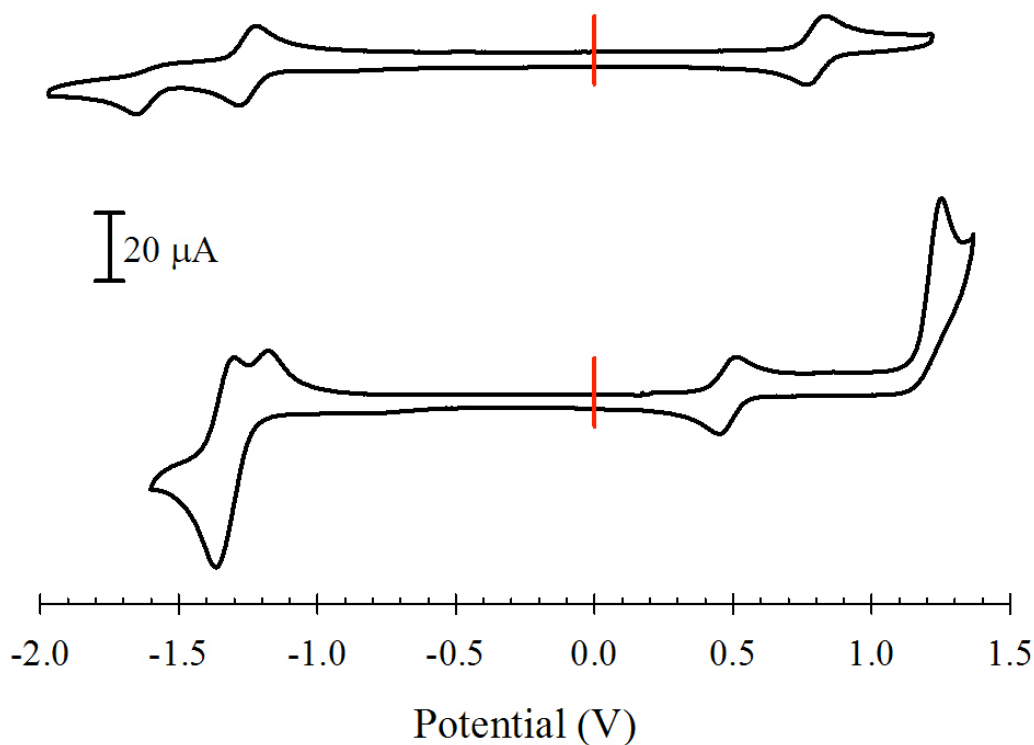


Figure 10. Cyclic Voltammograms for *mer,cis*-Re(tpy- κ^3 N)(CO)₂Cl (**1**; bottom) and *mer,cis*-[Re(tpy- κ^3 N)(CO)₂(PEt₃)]⁺ (**7**; top).

Intuitively, one might expect that the extended π -network of the terpyridine would result in lower reduction potentials relative to the bipyridine as a result of greater π -acidity. This is indeed observed. However, the data clearly indicate the profound influence the dicarbonyl terpyridine system has relative to the tricarbonyl bipyridine system in stabilizing the lower oxidation state of rhenium. The Re^I/Re^{II} oxidation for the *mer,cis*-Re(tpy- κ^3 N)(CO)₂Cl (**1**)

occurs 0.85 V less oxidizing than the *fac*-Re(bipyridine)(CO)₃Cl complex and is reversible. The *mer,cis*-Re(tpy-κ³N)(CO)₂Cl (**1**) first oxidation peak is also considered to be a one electron process (see Appendix C). Although the ligand set is quite extensive for the study at hand, similar observations are reached in analyzing these complexes in the manner described above. For example, the cyclic voltammogram for *mer,cis*-[Re(tpy-κ³N)(CO)₂(PEt₃)]⁺ (**7**) is shown in the top portion of Figure 10. Hori and co-workers³⁵ reported the electrochemical potentials for the *fac*-Re(bpy)(CO)₃(PEt₃)⁺ as -1.39 V, -1.94 V, and 1.6 V. The first reduction is bipyridine-based and reversible, followed an irreversible reduction (presumably, metal-based).²⁹ The oxidation is irreversible and is attributed to the one-electron oxidation of Re^I to Re^{II} which is followed by the rapid loss of CO. For the *mer,cis*-[Re(tpy-κ³N)(CO)₂(PEt₃)]⁺ (**7**) a one-electron, reversible oxidation wave is observed at +0.84 V and is assigned as a metal-based oxidation. Similarly, two reduction potentials are observed at -1.21 V and -1.64 V. The first reduction potential appears to be a reversible, one-electron reduction based on the reversible, one-electron oxidation at +0.84 V. The second reduction peak is irreversible. As mentioned previously, the first reduction potential is relatively invariant over the series of complexes. Thus, we attribute this potential to ligand-centered (terpyridine) reduction. The second irreversible wave at -1.64 V is a metal-based reduction.

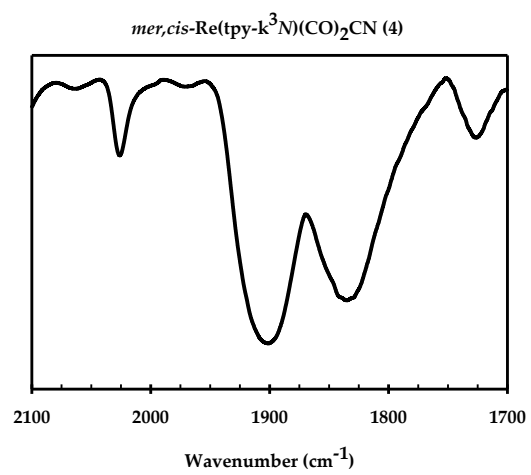
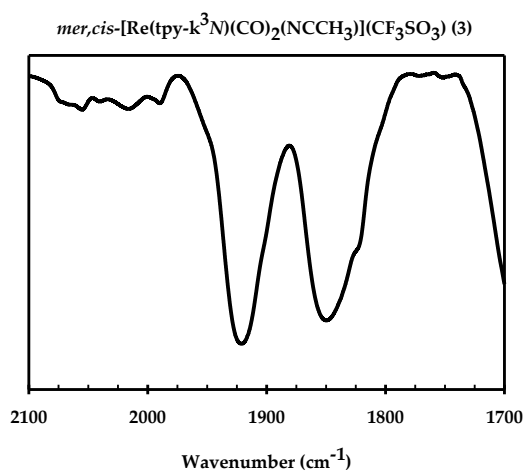
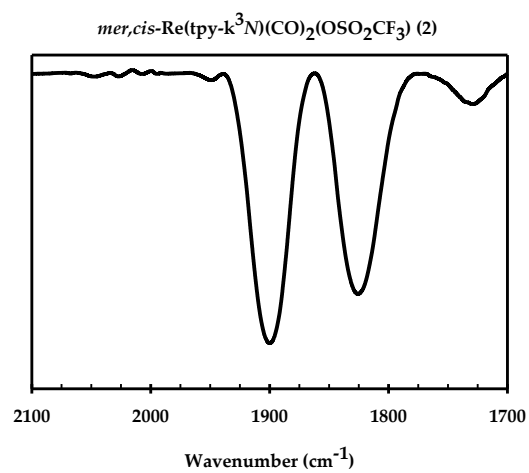
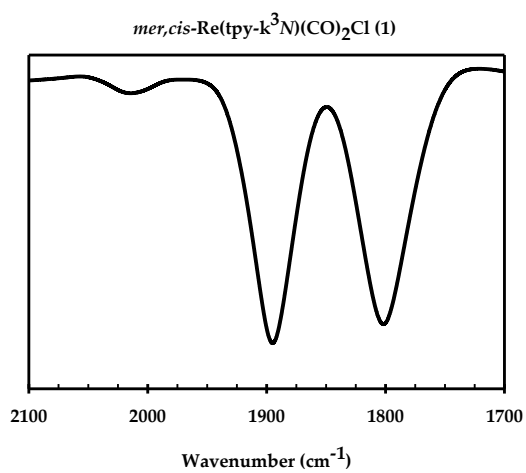
Again, the data clearly indicate the profound influence the dicarbonyl terpyridine system has relative to the tricarbonyl bipyridine system in stabilizing the lower oxidation state of rhenium. The $\text{Re}^{\text{I}}/\text{Re}^{\text{II}}$ oxidation for the *mer,cis*- $[\text{Re}(\text{tpy}-\kappa^3\text{N})(\text{CO})_2(\text{PEt}_3)]^+$ (**7**) occurs reversibly at a potential 0.84 V less oxidizing than the *fac*- $[\text{Re}(\text{bpy})(\text{CO})_3(\text{PEt}_3)]^+$ complex.

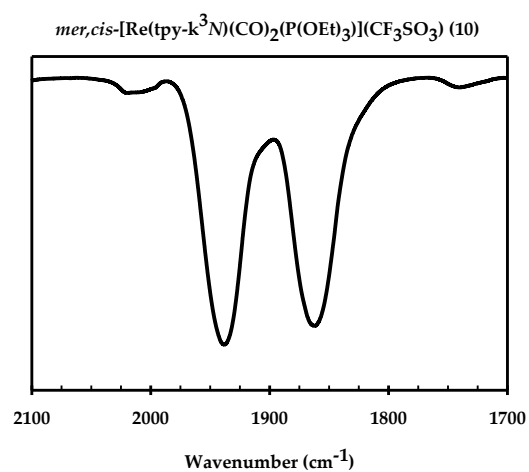
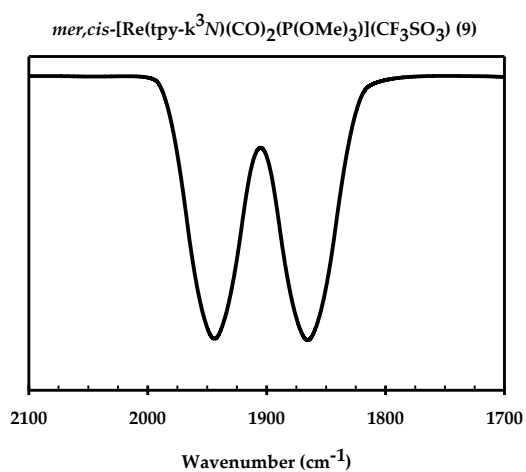
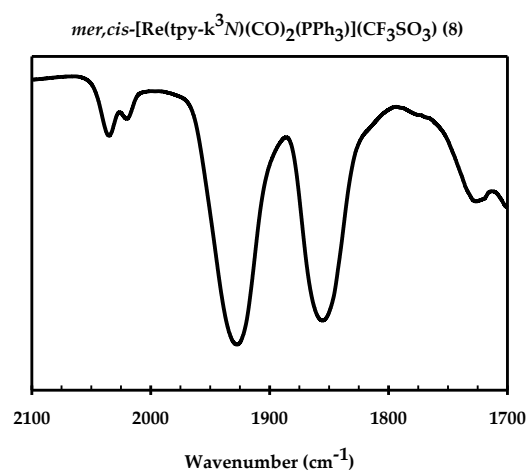
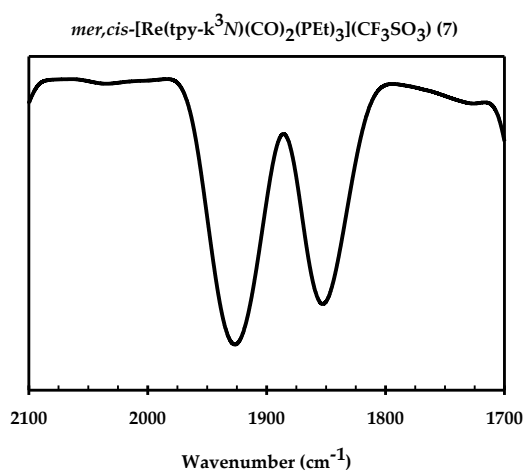
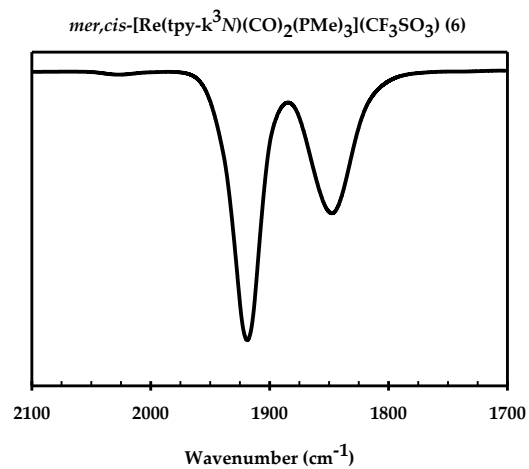
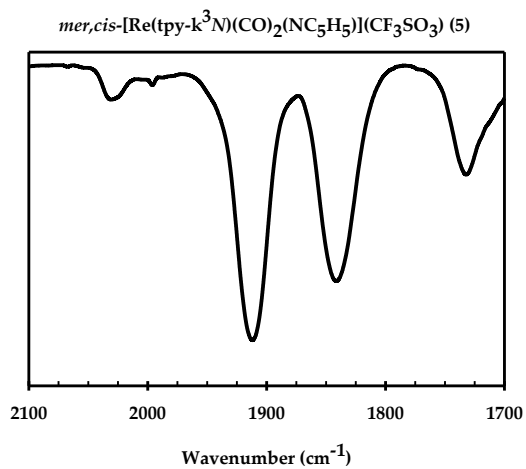
3.7 Summary

A series of meridionally-coordinated tridentate terpyridine rhenium(I) dicarbonyl complexes has been prepared and characterized. For the series of complexes the extended π -network of the terpyridine is observed to stabilize the lower oxidation state of rhenium. Many of the complexes absorb light throughout a significant portion of the visible spectrum. No room temperature luminescence is observed for any of the complexes presumably because the terpyridine bite angles are less than 90° resulting in a distorted octahedral geometry about the rhenium metal. These properties make the meridionally-coordinated tridentate terpyridine rhenium(I) dicarbonyl complexes interesting candidates for further studies.

APPENDICES

APPENDIX A: INFRARED SPECTRA





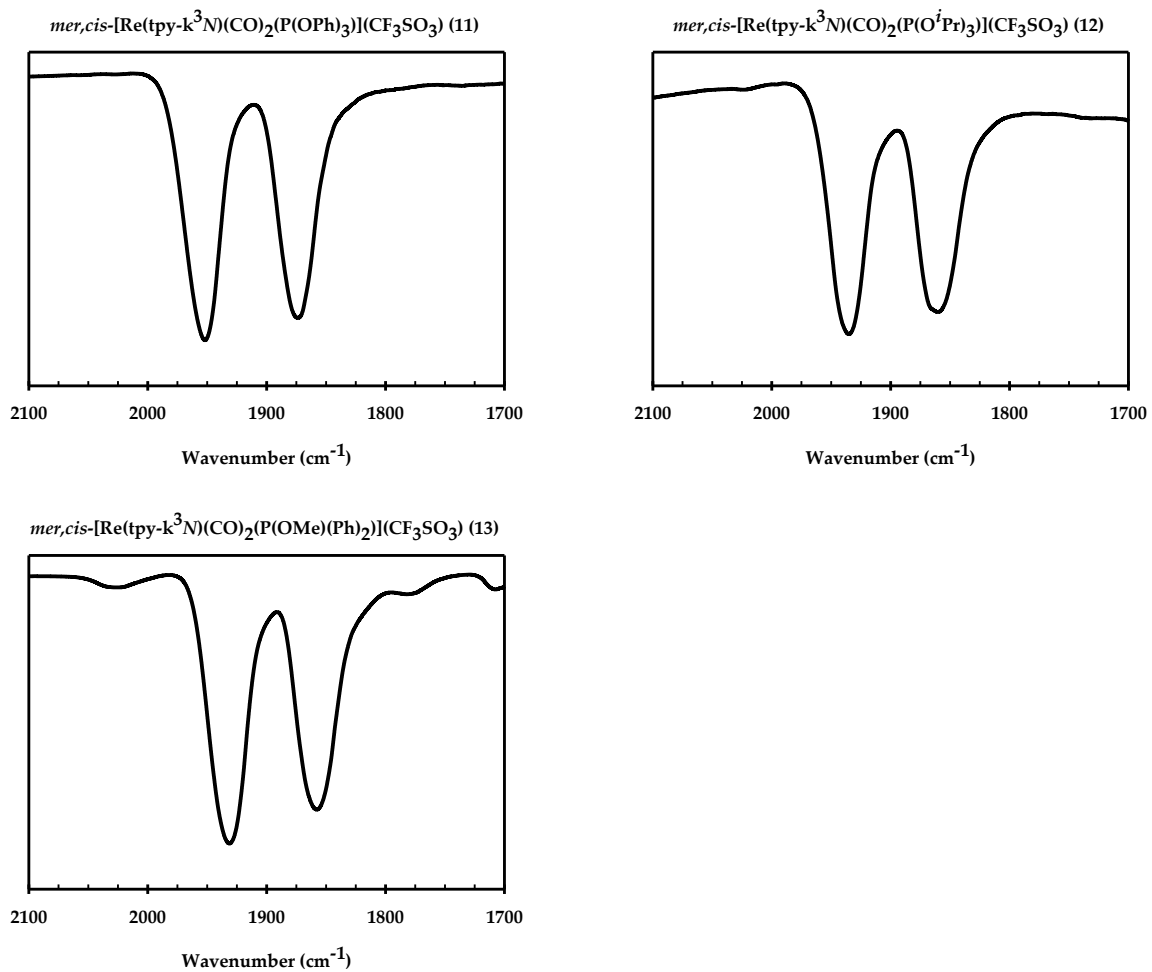


Figure 11. Infrared Spectra of Complexes 1–13 in the carbonyl region between 2200–1700 cm^{-1} .

APPENDIX B: NMR SPECTRA

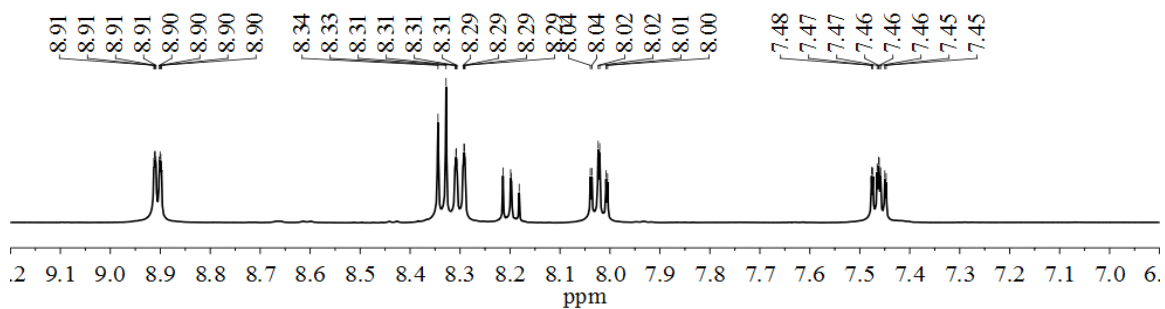


Figure 12. ^1H NMR of *mer,cis*- $\text{Re}(\text{tpy-}\kappa^3\text{N})(\text{CO})_2\text{Cl}$ (1) in $\text{DMSO-}d_6$.

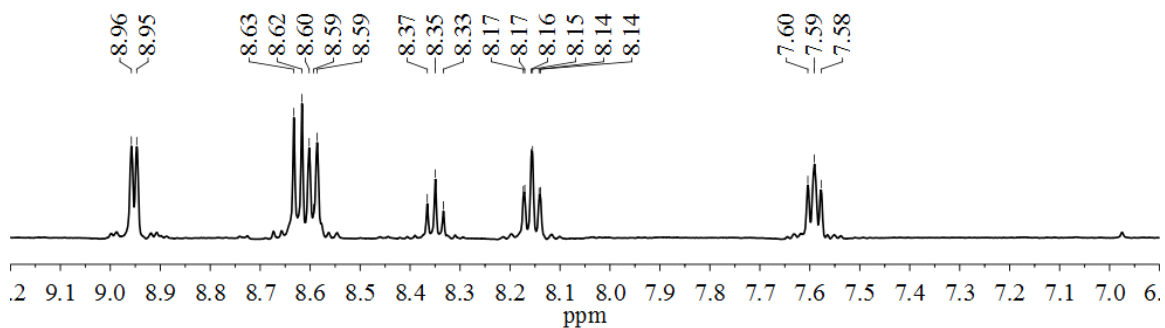


Figure 13. ^1H NMR of *mer,cis*- $\text{Re}(\text{tpy-}\kappa^3\text{N})(\text{CO})_2(\text{OSO}_2\text{CF}_3)$ (2) in $\text{DMSO-}d_6$.

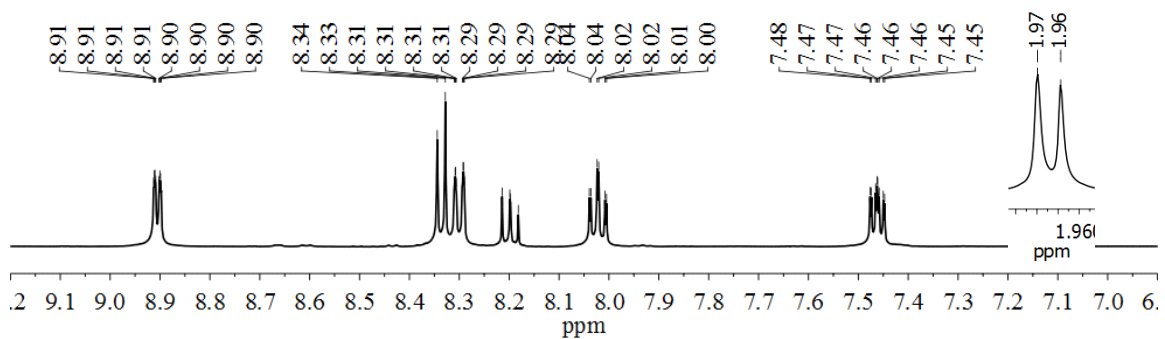


Figure 14. ^1H NMR of *mer,cis*- $[\text{Re}(\text{tpy-}\kappa^3\text{N})(\text{CO})_2(\text{CH}_3\text{CN})]^+\text{CF}_3\text{SO}_3^-$ (3) in acetonitrile- d_3 .

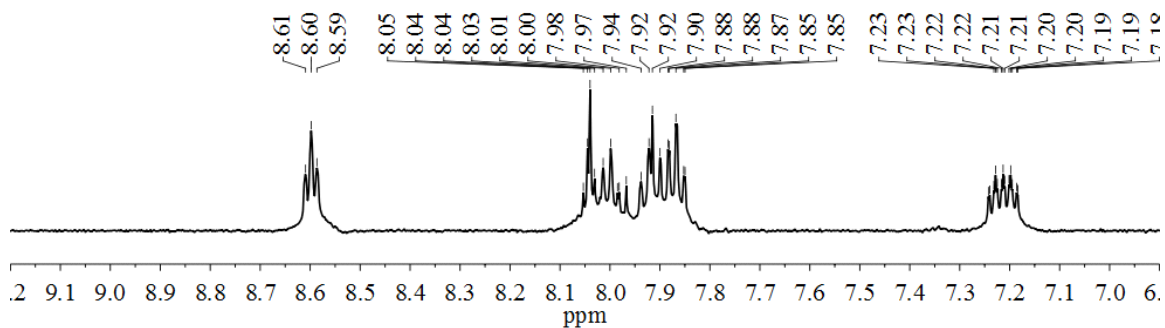


Figure 15. ^1H NMR of *mer,cis*- $\text{Re}(\text{tpy-}\kappa^3\text{N})(\text{CO})_2(\text{CN})(4)$ in acetonitrile- d_3 .

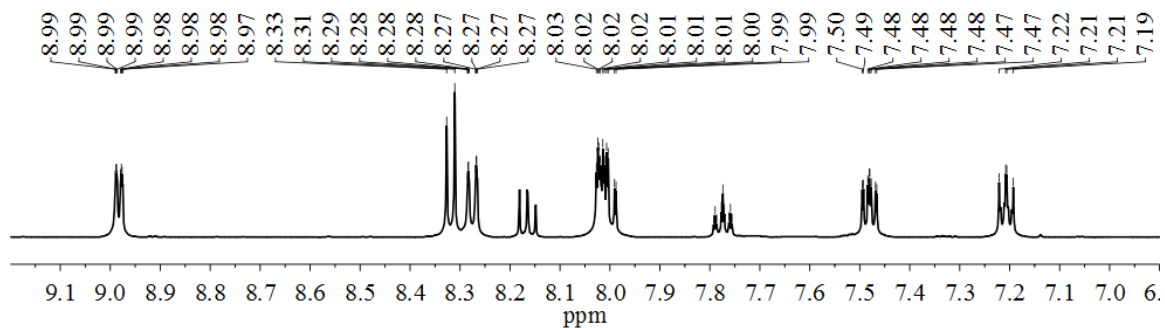


Figure 16. ^1H NMR of *mer,cis*- $[\text{Re}(\text{tpy-}\kappa^3\text{N})(\text{CO})_2(\text{NC}_5\text{H}_5)]^+\text{CF}_3\text{SO}_3^-$ (5) in acetonitrile- d_3 .

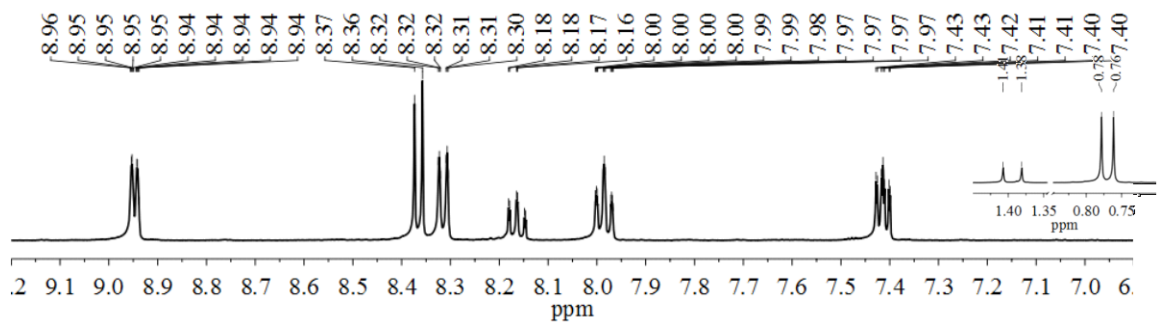


Figure 17. ^1H NMR of *mer,cis*- $[\text{Re}(\text{tpy-}\kappa^3\text{N})(\text{CO})_2(\text{PMe}_3)]^+\text{CF}_3\text{SO}_3^-$ (6) in acetonitrile- d_3 .

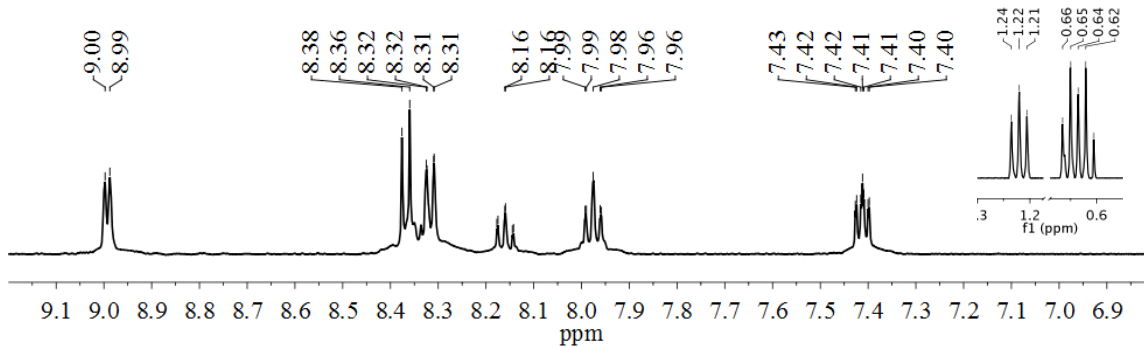


Figure 18. ^1H NMR of *mer,cis*-[Re(tpy- $\kappa^3\text{N}$)(CO) $_2$ (PEt $_3$)] $^+\text{CF}_3\text{SO}_3^-$ (7) in acetonitrile- d_3 .

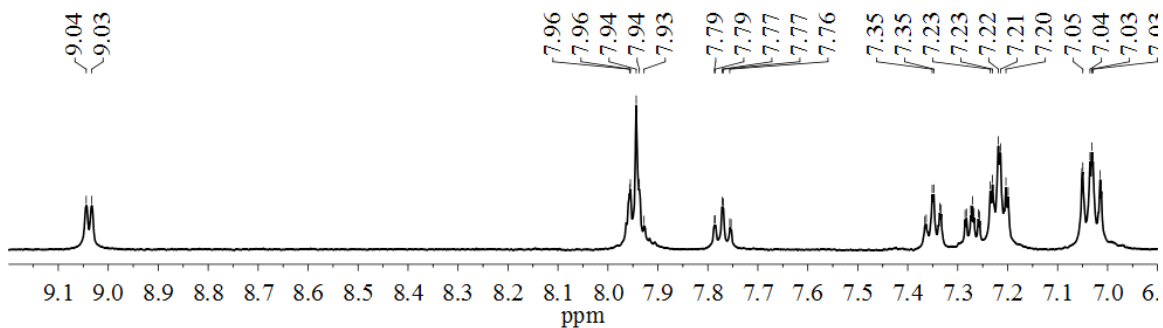


Figure 19. ^1H NMR of *mer,cis*-[Re(tpy- $\kappa^3\text{N}$)(CO) $_2$ (PPh $_3$)] $^+\text{CF}_3\text{SO}_3^-$ (8) in acetonitrile- d_3 .

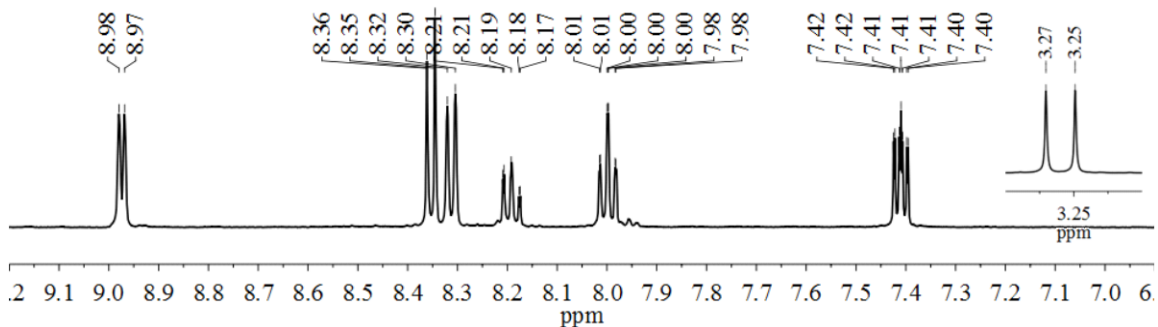


Figure 20. ^1H NMR of *mer,cis*-[Re(tpy- $\kappa^3\text{N}$)(CO) $_2$ (P(OMe) $_3$)] $^+\text{CF}_3\text{SO}_3^-$ (9) in acetonitrile- d_3 .

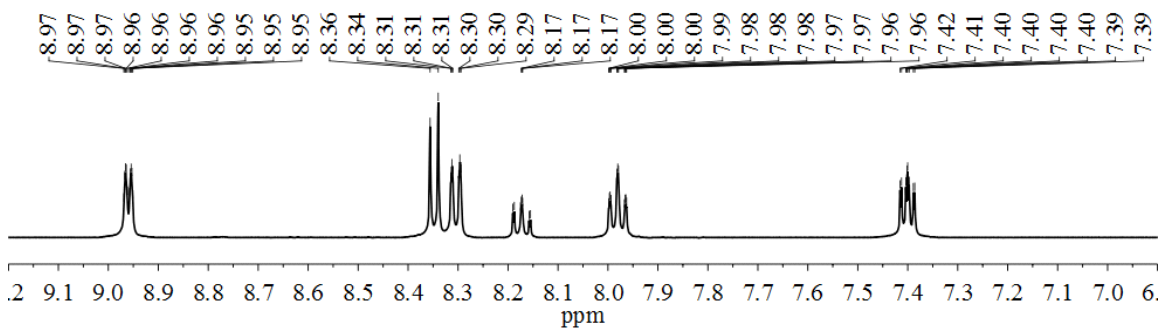


Figure 21. ^1H NMR of *mer,cis*-[Re(tpy- $\kappa^3\text{N}$)(CO) $_2$ (P(OEt) $_3$)] $^+\text{CF}_3\text{SO}_3^-$ (10) in acetonitrile- d_3 .

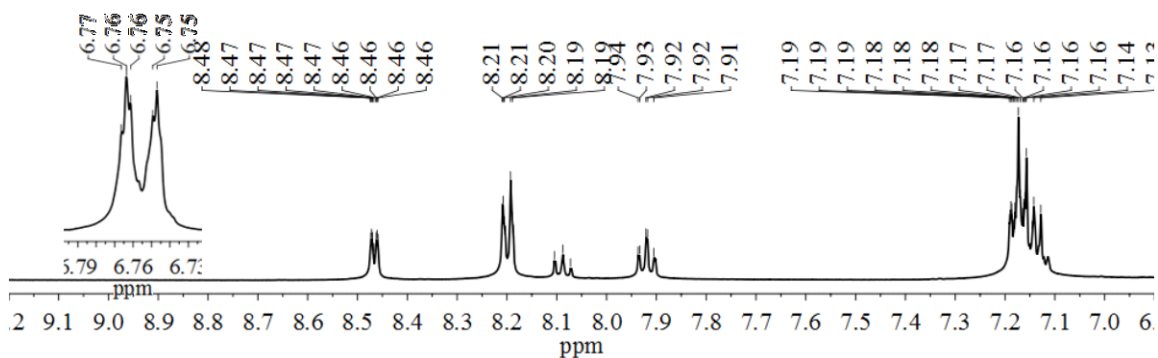


Figure 22. ^1H NMR of $\text{mer,cis-}[\text{Re}(\text{tpy-}\kappa^3\text{N})(\text{CO})_2(\text{P}(\text{OPh})_3)]^+\text{CF}_3\text{SO}_3^-$ (11) in acetonitrile- d_3 .

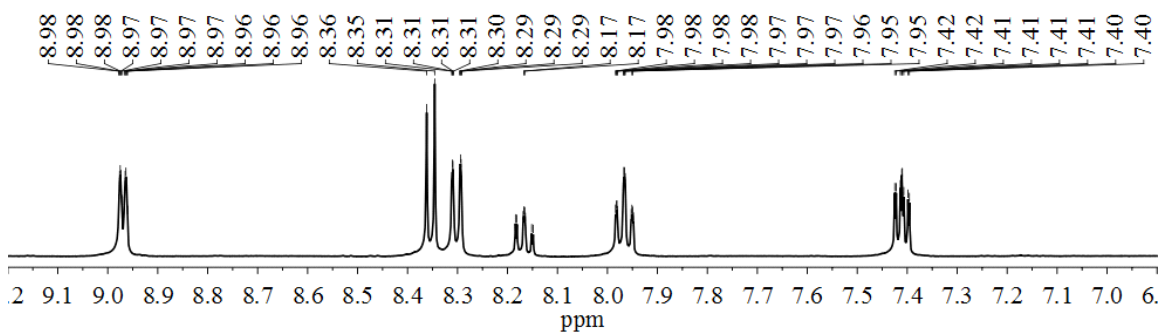


Figure 23. ^1H NMR of $\text{mer,cis-}[\text{Re}(\text{tpy-}\kappa^3\text{N})(\text{CO})_2(\text{P}(\text{O}i\text{Pr})_3)]^+\text{CF}_3\text{SO}_3^-$ (12) in acetonitrile- d_3 .

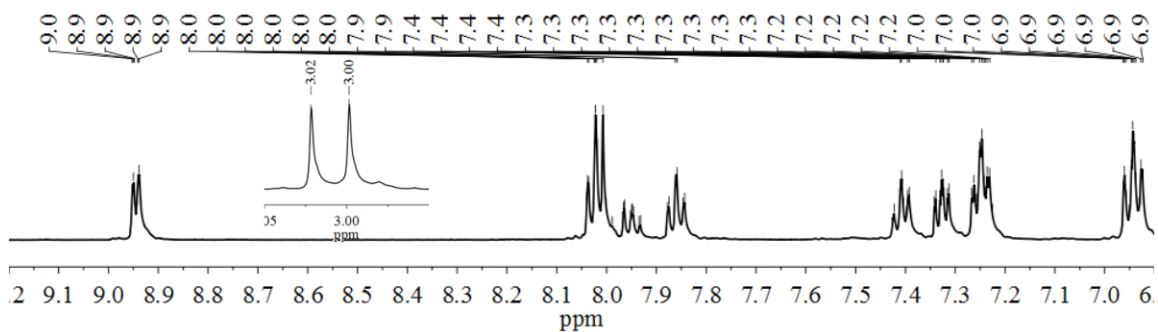


Figure 24. ^1H NMR of $\text{mer,cis-}[\text{Re}(\text{tpy-}\kappa^3\text{N})(\text{CO})_2(\text{P}(\text{OMe})(\text{Ph})_2)]^+\text{CF}_3\text{SO}_3^-$ (13) in acetonitrile- d_3 .

APPENDIX C: DETERMINING ELECTROCHEMICAL REVERIBLITY

The number of electrons involved in the first oxidation for *mer,cis*-Re(tpy- κ^3N)(CO)₂Cl was calculated by plotting the peak current (i_p) versus the square root of scan rate, providing a linear regression line which confirms i_p is independent of scan rate. The equation provides by the linear regression line can then be directly related to the Randles-Sevcik equation,

$$i_p = (2.69 \times 10^5)n^{3/2}A D^{1/2}C_o v^{1/2} \quad 1.1$$

where i_p is the peak current measured from the baseline, n is the number of electrons involved in the redox peak, A is the area of the working electrode, D is the diffusion coefficient, C_o is the concentration of analyte, and v is scan rate.

Table 3 provides the data used for the plot and Figure 25 shows the linear regression line ($y = 78118x - 0.0856$).

Using decamethylferrocene as a standard, which is a one electron redox couple (Fe^{2+}/Fe^{3+})¹, for the estimation of the number of electrons in the first oxidation peak of *mer,cis*-Re(tpy- κ^3N)(CO)₂Cl. The same plot (i_p vs. $v^{1/2}$) for decamethylferrocene was created (Table 2 Figure 2) producing a linear regression line ($y = 170803x - 0.0841$). In order to find the number of electrons in the first

¹ Connelly, N. G.; Geiger, W.E. *Chem Rev.* **1996**, 96, 877-910

oxidation peak of *mer,cis*-Re(tpy-κ³N)(CO)₂Cl using the Randles-Sevcik equation we assumed the diffusion coefficient of *mer,cis*-Re(tpy-κ³N)(CO)₂Cl and decamethylferrocene are the same, and because the same working electrode was used to perform these measurements *A* can be set to equal 1. With these assumptions the Randles-Sevcik equation is reduced to the Equation 1.2.

$$i_p = (2.69 \times 10^5)n^{3/2}C_o v^{1/2} \quad 1.2$$

Using the coefficient of *x* from the linear regression equation of both complexes we then divided by the concentration of each complex and 2.69 × 10⁵ giving the following values for both complexes setting the value equal to *n* (negating the 3/2): *mer,cis*-Re(tpy-κ³N)(CO)₂Cl (1.174 × 10⁻⁴ M)

$$\frac{78118}{(2.69 \times 10^5)(1.174 \times 10^{-4})} = n$$

$$2473.6 = n$$

decamethylferrocene (2.819 × 10⁻⁴)

$$\frac{170803}{(2.69 \times 10^5)(2.819 \times 10^{-4})} = n$$

$$2197.0 = n$$

for decamethylferrocene *n* equals 1. Using the values from equation 1.2 for both complexes the following equation will give the number of electrons involved in first oxidation of *mer,cis*-Re(tpy-κ³N)(CO)₂Cl,

$$2473.6 n = 2197.0$$

$$\frac{2473.6}{2197.0} = n$$

$$n = 1.12$$

which is slightly greater than one electron but the first oxidation of *mer,cis*- $\text{Re}(\text{tpy}-\kappa^3\text{N})(\text{CO})_2\text{Cl}$ can still be considered a one electron redox couple.

Table 3. Peak current, scan rates and square root of scan rates of *mer,cis*- $\text{Re}(\text{tpy}-\kappa^3\text{N})(\text{CO})_2\text{Cl}$.

i_p (A)	Scan rate (V/s)	$v^{1/2}$
2.96×10^{-5}	5	2.24
2.76×10^{-5}	4.5	2.12
2.64×10^{-5}	4	2.00
2.48×10^{-5}	3.5	1.87
2.38×10^{-5}	3	1.73
2.20×10^{-5}	2.5	1.58
1.91×10^{-5}	2	1.41
1.71×10^{-5}	1.5	1.22
1.41×10^{-5}	1	1.00
1.25×10^{-5}	0.75	0.87
1.00×10^{-5}	0.5	0.71
6.90×10^{-5}	0.25	0.50

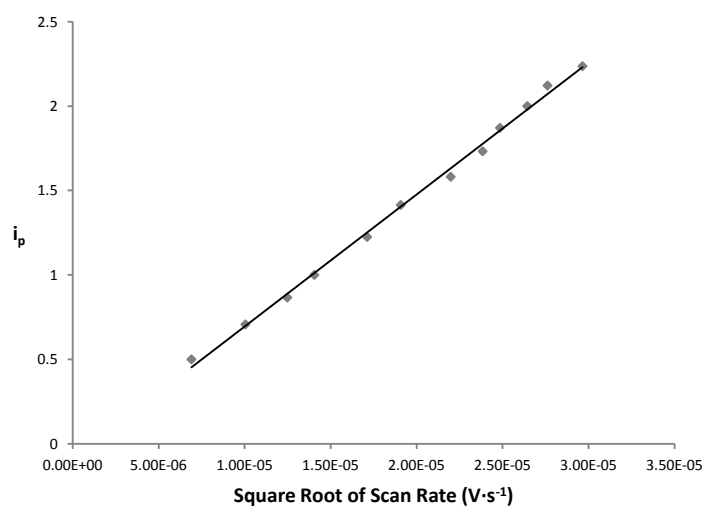


Figure 25. Randles-Sevcik plot of mer,cis-Re(tpy-κ³N)(CO)₂Cl with a coefficient of determination value of 0.9969.

Table 4. Peak current, scan rates and square root of scan rates of decamethylferrocene.

i_p (A)	Scan rate	
	(V/s)	$\nu^{1/2}$
1.35×10^{-5}	5	2.24
1.29×10^{-5}	4.5	2.12
1.20×10^{-5}	4	2.00
1.16×10^{-5}	3.5	1.87
1.06×10^{-5}	3	1.73
9.84×10^{-5}	2.5	1.58
8.98×10^{-5}	2	1.41
7.80×10^{-5}	1.5	1.22
6.39×10^{-5}	1	1.00
5.56×10^{-5}	0.75	0.87
4.53×10^{-5}	0.5	0.71
3.31×10^{-5}	0.25	0.50

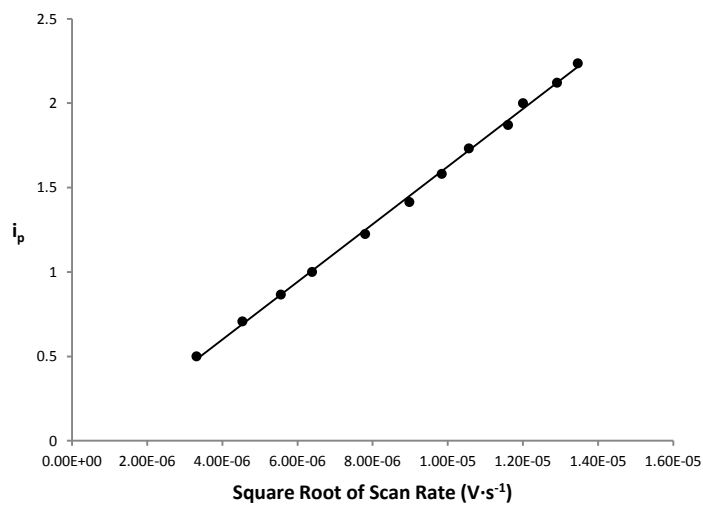


Figure 26. Randles-Sevcik plot of decamethylferrocene with a coefficient of determination value of 0.9986.

REFERENCES

1. Montalti, M.; Cedi, A.; Prodi, L.; Gandolfi, M. T. *Handbook of Photochemistry*, 3rd ed.; CRC press: Boca Raton, 2006.
2. Schubert, U. S.; Hofmeier, H.; Newkome, G. R. *Modern Terpyridine Chemistry*, 1st ed.; Wiley-VCH: Weinheim, 2006.
3. Constable, E. C. *Chem. Soc. Rev.* **2007**, 36, 246.
4. Cooke, M. W.; Hanan, G. S. *Chem. Soc. Rev.* **2007**, 36, 1466.
5. Medlycott, E. A.; Hanan, G. S. *Chem. Soc. Rev.*, **2005**, 34, 133.
6. Andres, P.R.; Schubert, U. S. *Adv. Mater.* **2004**, 16, 1043.
7. Heller, M.; Schubert, U. S. *Eur. J. Org. Chem.* **2003**, 947.
8. Hofmeier, H.; Schubert, U. S. *Chem. Soc. Rev.* **2004**, 33, 373.
9. Altobello, S.; Argazzi, R.; Caramori, S.; Contado, C.; Da Fre, S.; Rubino, P.; Chone, C.; Larramona, G.; Bignozzi, C. A.; *J. Am. Chem. Soc.* **2005**, 127, 15342.
10. O'Regan, B.; Grätzel, M. *Nature* **1991**, 353, 737.
11. Ghosh, S.; Chaitanya, G. K.; Bhanuprakash, K.; Nazeeruddin, M. K., Grätzel, M.; Reddy, P. Y. *Inorg. Chem.* **2006**, 45, 7600.
12. Hagemann, O.; Jørgensen, M.; Krebs, F. C.; *J. Org. Chem.* **2006**, 71, 5546.
13. Rawling, T.; Austin, C.; Buchholz, F.; Colbran S. B.; McDonagh, A. M. *Inorg. Chem.* **2009**, 48, 3215.
14. Concepcion, J. J.; Jurss, J. W.; Norris, M. R.; Chen, Z. F.; Templeton, J. L.; Meyer, T. J. *Inorg. Chem.* **2010**, 49, 1277.
15. Wasylenko, D. J.; Ganesamoorthy, C.; Koivisto, B. D.; Henderson M. A.; Berlinguette, C. P.; *Inorg. Chem.* **2010**, 49, 2202.
16. Ehrenschwender, T.; Barth, A.; Puchta, H.; Wagenknecht, H. *Org. Biomol. Chem.* **2012**, 10, 46.
17. Liu, P.; Zhou, C.; Xiang, S.; Che, C. *Chem. Commun.* **2010**, 46, 2739.
18. Chen, X.; Liu, Q.; Sun, H.; Yu, X.; Pu, L. *Tetrahedron Lett.* **2010**, 51, 2345.
19. Wild, A.; Winter, A.; Schlütter, F.; Schubert, U. S. *Chem. Soc. Rev.* **2011**, 40, 1459.

20. Kirgan, R. A.; Sullivan, B. P.; Rillema, D. P. *Top. Curr. Chem.* **2007**, 281, 45.
21. Kalyanasundaram, K. *Photochemistry of Polypyridine and Porphyrin Complexes*; Academic Press: London, 1992.
22. Scandola, F.; Indelli, M. T.; Chiorboli, C.; Bignozzi, C. A. *Top. Curr. Chem.* **1990**, 158, 73.
23. Sullivan, B. P.; Krist, H. E.; Guard, H. E. *Electrochemical and Electrocatalytic Reactions of Carbon Dioxide*; Elsevier: Amsterdam, 1992.
24. Arakawa, H.; Aresta, M.; Armor, J. N.; Barteau, M. A.; Beckman, E. J.; Bell, A. T.; Bercaw, J. E.; Creutz, C.; *et al.* *Chem. Rev.* **2001**, 101, 953.
25. Meyer, G. J. *Progress in Inorganic Chemistry: Molecular Level Artificial Photosynthetic Materials, Vol. 44*; John Wiley & Sons, Inc.: New York, 1997.
26. Alstrum-Acevedo, J. H.; Brennaman; M. K. Meyer, T. J. *Inorg. Chem.* **2005**, 44, 6802.
27. Meyer, T. J. *Acc. Chem. Res.* **1989**, 22, 163.
28. Balzani, V.; Scandola, F. *Supramolecular Photochemistry*; Ellis Horwood: London, 1991.
29. Ramamurthy, V.; Schanze, K. S. *Semiconductor Photochemistry and Photophysics, Vol. 10*; Marcel Dekker, Inc.: New York, 2003.
30. Grätzel, M. *Nature* **2001**, 414, 338.24
31. Yella, A.; Lee, H-W.; Tsao, H. N.; Yi, C.; Chandrin, A. K.; Nazeeruddin, M. K.; Diau, E.W-G.; Yeh, C. Y.; Zakeeruddin, S. M.; Grätzel, M. *Nature* **2011**, 334, 629.
32. Lo, K.K-W.; Ng, D C-M; Hui, W-K.; Cheung, K-K. *J. Chem. Soc., Dalton Trans.*, **2001** 18, 2634.
33. Amoroso, A. J.; Arthur, R. J.; Coogan, M. P. ; Court J. B.; Fernandez-Moreira, V.; Hayes A. J.; Lloyd, D.; Millet C.; Pope, S. J. A. *New J. Chem.*, **2008**, 32, 1097.
34. Caspar, J. V.; Meyer, T. J. *J. Phys. Chem.* **1983**, 87, 952.
35. Hori, H.; Koike, K.; Ishizuka, M.; Takeuchi, K.; Ibusuki, T.; Ishitani, O. *J. Organomet. Chem.* **1997**, 530, 169.
36. Takeda, H.; Koike, K.; Inoue, H.; Ishitani, O.; *J. Am. Chem. Soc.* **2008**, 130, 2023.
37. Worl, L. A.; Duesing, R.; Chen, P.; Ciana, L. D.; Meyer, T. J. *J. Chem. Soc., Dalton Trans.* **1991**, 849-858.
38. Rodriguez, A. M. B.; Gabrielsson, A.; Motevalli, M.; Matousek, P.; Towrie, M.; Sebera, J.; Zalis, S.; Anntonin. Vlcek, J. *J. Phys. Chem. A* **2005**, 109, 5016-5025.
39. Leasure, R. M.; Sacksteder, L.; Nesselrodt, D.; Reitz, G. A.; Demas, J. N.; DeGraff, B. A. *Inorg. Chem.* **1991**, 30, 3722-3728.

40. Amoroso, A. J.; Banu, A.; Coogan, M. P.; Edwards, P. G.; Hossain, G.; Malik, K. M. A. *Dalton Trans.* **2010**, 39, 6993.
41. Ge, Q.; Corkery, C. T.; Humphrey, M. G.; Samoc, M.; Hor, A.; *Dalton Trans.* **2009**, 31, 6192.
42. Coogan, M. P.; Fernandez-Moreira, V.; Kariuki, B. M.; Pope, S.; Thorp-Greenwood, F. L. *Angew. Chem.*, **2009**, 48, 4965.
43. Machura, B.; Kruszynski, R.; Kusz, J. *Inorg. Chem. Commun.* **2007**, 10, 918.
44. Metcalfe, C.; Rajput, C.; Thomas, Jim A. *J. of Inorg. Biochem.* **2006**, 100, 1314.
45. Freyer, A.; Freyer, A.; DiMeglio, C. *J. of Chem. Educ.* **2006**, 83, 788.
46. Moya, S. A.; Pastene, R.; Le Bozec, H.; Baricelli, P. J.; Pardey, A. J.; Gimeno, J. *Inorganica Chimica Acta* **2001**, 312, 7.
47. Gelling, A.; Olsen, M. D.; Orrell, K. G.; Osborne, A. G.; Sik, V. *J. Chem. Soc., Dalton Trans.: Inorganic Chemistry* **1998**, 20, 3479.
48. Fernandez-Moreira, V.; Thorp-Greenwood, F. L.; Arthur, R. J.; Kariuki, B. M.; Jenkins, R. L.; Coogan, M. P. *Dalton Trans.* **2010**, 39, 7493.
49. Abel, E. W.; Dimitrov, V. S.; Long, N. J.; Orrell, K. G.; Osbourne, A. G.; Pain, H. M.; Sik, V.; Hursthouse, M. B.; Mazid, M. A. *J. Chem. Soc., Dalton Trans.* **1993**, 4, 597.
50. Chang, L.; Rall, J.; Tisato, F.; Deutsch, E.; Heeg, M. J. *Inorg. Chim. Acta* **1993**, 205, 35.
51. Helberg, L. E.; Barrera, J.; Sabat, M.; Harman, W. D. *Inorg. Chem.* **1995**, 34, 2033.
52. Machura, B.; Kruszynski, R.; Kusz, J. *Inorg. Chem. Comm.* **2007**, 10, 918
53. Rall, J.; Weingart, F.; Ho, D. M.; Heeg, M. J.; Tisato, F.; Deutsch, E. *Inorg. Chem.* **1994**, 33, 3442.
54. P. L. Feist, *J. Chem. Edu.* **2001**, 78, 351
55. For example, we used a Pressure Monitor and Purging QianCap from Q Lab Tech.
56. Smithback, J. L.; Helms, J. B.; Woessner, S. M.; Sullivan, B. P. *Inorg. Chem.* **2006**, 45(5), 2163.
57. Koike, K.; Tanabe, J.; Toyama, S.; Tsubaki, H.; Sakamoto, K.; Westwell, J. R.; Johnson, F. P. A.; Hori, H.; Saitoh, H.; Ishitani, O. *Inorg. Chem.* **2000**, 39(13), 2777.
58. Bartik, T.; Himmler, T.; Schulte, H. G.; Seevogel, K. *J. Organomet. Chem.* **1984**, 272, 29.
59. Crabtree, R. H. *The Organometallic Chemistry of the Transition Metals*, 5th ed.; Wiley: Hoboken, 2009.
60. Tolman, C. A. *Chem. Reviews* **1977**, 77(3), 313.
61. Monat, J. E.; Rodriguez, J. H.; McCusker, J. K. *J. Phys. Chem. A* **2002**, 106, 7399.

62. Kurz, P.; Probst, B.; Spingler, B.; Alberto, R. *Eur. J. Inorg. Chem.* **2006**, 2966.
63. Kalyanasundaram, K.; Grätzel, M.; Nazeeruddin, Md. K. *Inorg. Chem.* **1992**, 31, 5243.
64. Juris, A.; Campagna, S.; Bidd, I.; Lehn, J-M.; Ziessel, R. *Inorg. Chem.*, **1988**, 27, 4007.
65. Fujita, E.; Brunschwig, B. S. *Homogeneous Redox Catalysis in CO₂ Fixation in Electron Transfer in Chemistry*, (Balzani, V., Ed.); Wiley-VCH Verlag GmbH, Weinheim, Germany, 2008.